View Article Online / Journal Homepage / Table of Contents for this issue
Dynamic Article Links

PCCP

Cite this: *Phys. Chem. Chem. Phys.*, 2011, **13**, 18264–18287

www.rsc.org/pccp

PERSPECTIVE

Published on 19 September 2011. Downloaded by BELGIAN INSTITUTE FOR SPACE AERONOMY on 11/02/2016 11:00:19.

Doubly-charged ions in the planetary ionospheres: a review

Roland Thissen,*[a] Olivier Witasse,[b] Odile Dutuit,[ac] Cyril Simon Wedlund,[d] Guillaume Gronoff[e] and Jean Lilensten[a]

Received 15th June 2011, Accepted 22nd August 2011
DOI: 10.1039/c1cp21957j

This paper presents a review of the current knowledge on the doubly-charged atomic and molecular positive ions in the planetary atmospheres of the Solar System. It is focused on the terrestrial planets which have a dense atmosphere of N_2 or CO_2, *i.e.* Venus, the Earth and Mars, but also includes Titan, the largest satellite of Saturn, which has a dense atmosphere composed mainly of N_2 and a few percent of methane. Given the composition of these neutral atmospheres, the following species are considered: C^{++}, N^{++}, O^{++}, CH_4^{++}, CO^{++}, N_2^{++}, NO^{++}, O_2^{++}, Ar^{++} and CO_2^{++}. We first discuss the status of their detection in the atmospheres of planets. Then, we provide a comprehensive review of their complex and original photochemistry, production and loss processes. Synthesis tables are provided for those ions, while a discussion on individual species is also provided. Methods for detecting doubly-charged ions in planetary atmospheres are presented, namely with mass-spectrometry, remote sensing and fine plasma density measurements. A section covers some original applications, like the possible effect of the presence of doubly-charged ions on the escape of an atmosphere, which is a key topic of ongoing planetary exploration, related to the evolution of a planet. The results of models, displayed in a comparative way for Venus, Earth, Mars and Titan, are discussed, as they can predict the presence of doubly-charged ions and will certainly trigger new investigations. Finally we give our view concerning next steps, challenges and needs for future studies, hoping that new scientific results will be achieved in the coming years and feed the necessary interdisciplinary exchanges amongst different scientific communities.

[a] *Institut de Planétologie et d'Astrophysique de Grenoble, UJF-Grenoble 1/CNRS-INSU, UMR 5274, Grenoble, F-38041, France. E-mail: Roland.thissen@obs.ujf-grenoble.fr*
[b] *Research and Scientific Support Department of the European Space Agency, ESTEC, PO BOX 299, 2200 AG Noordwijk, The Netherlands*
[c] *Space Research Institute, Austrian Academy of Sciences (IWF/OAW), Schmiedlstraße 6, 8042 Graz, Austria*
[d] *Belgian Institute for Space Aeronomy BIRA-IASB, Brussels, Belgium*
[e] *Science Directorate, Chemistry and Dynamics Branch, NASA Langley Research Center, Hampton, VA, USA*

Roland Thissen

Roland Thissen obtained his PhD in photoinduced chemistry of molecular dications in 1993 at the Liège University (Belgium). After post-doctoral positions in Liège, Japan (Tsukuba) and France (Orsay), he became in 1999 CNRS researcher, in Laboratoire de Chimie Physique, Paris Sud University. He developed the chemistry applications of the CERISES instrument linked to Synchrotron radiation, associating state selection and ion molecule reactivity. He moved to Laboratoire de Planétologie de Grenoble in 2007 to develop a high resolution mass spectrometer for Titan chemistry studies, and became, in 2011, responsible of the Planetary Science group of Institut de Planétologie et d'Astrophysique de Grenoble.

Olivier Witasse

Olivier Witasse obtained his PhD in physics of the ionospheres of the Earth and of Mars in 2000 at the University of Grenoble (France). After two post-doctoral positions in Noordwijk (The Netherlands) and Brussels, he became in 2003 staff member of the European Space Agency in Noordwijk. He works in the Solar System Missions division, as Project Scientist of the Mars Express mission. Besides his duty in the scientific management of planetary missions, he carries out research on the upper atmosphere of terrestrial planets.

This journal is © the Owner Societies 2011

View Article Online

Published on 19 September 2011. Downloaded by BELGIAN INSTITUTE FOR SPACE AERONOMY on 11/02/2016 11:00:19.

1. Introduction

In this paper, we propose a review of the present knowledge on the doubly-charged atomic and molecular positive ions in the planetary atmospheres of the Solar System. It is focused on the terrestrial planets which have a dense atmosphere of N_2 or CO_2, *i.e.* Venus, the Earth and Mars. It also includes Titan, the largest satellite of Saturn, which has a dense atmosphere composed mainly of N_2 and a few percent of methane.[1] Given the composition of these neutral atmospheres, the following species are considered: C^{++}, N^{++}, O^{++}, CH_4^{++}, CO^{++}, N_2^{++}, NO^{++}, O_2^{++}, Ar^{++} and CO_2^{++}. We should mention here that a population of doubly-charged ions, namely He^{++}, also called alpha particles, is present in significant amount (few percent of all ions) in the solar wind, which contains as well a minor abundance of multiply charged atoms.[2] These will not be discussed in this article, which deals only with ionospheres.

Due to the lack of laboratory measurements concerning their lifetime, their production by photons and electrons or their decay processes by dissociation, recombination or reactions with neutrals, the existence of doubly-charged ions in upper atmospheres has often been neglected up to now. It was commonly admitted that cross sections for double ionisation should be much smaller than for single ionisation in the photon and electron energy range available in upper atmospheres and that small diatomic or triatomic doubly-charged positive ions would have a short lifetime in atmospheric conditions. Moreover, as their detection both by remote or *in situ* methods is a real challenge, there was no way to check their existence and measure their density. However some satellite measurements have shown that atomic doubly-charged ions are present in the ionospheres of the Earth,[3–16] Venus[17,18] and Io.[19–21] Molecular doubly-charged ions have not been detected in any ionosphere so far, even if they

Odile Dutuit

Odile Dutuit obtained her Physical Chemistry PhD degree in 1978 at the University Paris-Sud. She was a post doctoral fellow in the laboratory of Professor Y. T. Lee in Berkeley, USA in 1982. She is Director of Research in CNRS. After being in the Laboratoire de Chimie Physique in Orsay (Paris-Sud University) for many years, she moved to Grenoble and became director of the Laboratoire de Planétologie de Grenoble from 2007 until 2010. Member of the Institut de Planétologie et d'Astrophysique de Grenoble, she is presently on sabbatical in the Institute for Space Science in Graz (Austrian Academy of Sciences), Austria. She is a physical chemistry experimentalist and works on the chemistry of planetary atmospheres.

Cyril Simon Wedlund

Cyril Simon Wedlund holds a PhD in Astrophysics from the University Joseph Fourier of Grenoble, France. He is currently working at BIRA/IASB in Brussels, Belgium where his main study is the tomographic optical observation of the Earth's aurora. His interests range from the modelling of solar energetic particles such as electrons and protons in the atmospheres of the Earth, Mars and Venus to the processes at the origin of airglow and aurora in the solar system, using space-borne (Cluster, DMSP, Mars Express) and ground-based (EISCAT, ALIS) instrumentation.

Guillaume Gronoff

Guillaume P. Gronoff holds a PhD in Astrophysics from the University Joseph Fourier of Grenoble, France and an engineer diploma from Polytechnique Grenoble. He is currently working in NASA Langley Research Center, Virginia, USA, where he uses airglow emissions measured by UV spectrometers on board space missions, such as Mars Express, to retrieve neutral atmospheric parameters. His areas of expertise cover many planetary upper atmospheres including Venus, Mars and Titan, and their corresponding airglow emissions. Specialist in numerical modelling, he was the first to consistently calculate the effects of electron precipitation and cosmic ray degradation in the atmosphere of Titan.

Jean Lilensten

Jean Lilensten is researcher in CNRS at IPAG where he conducts researches on the impact of the solar activity on the planetary upper atmospheres. He is Editor-in-Chief of the scientific journal Space Weather and Space Climate.

View Article Online

Published on 19 September 2011. Downloaded by BELGIAN INSTITUTE FOR SPACE AERONOMY on 11/02/2016 11:00:19.

have been predicted for more than 35 years to be present at Earth,[6,22–25] and more recently at Mars,[26,27] Titan[28] and Venus.[29] In recent years, significant progress has been made in laboratory measurements of the relevant photochemical data and parameters, in the design of space instrumentation, and in numerical models. In particular major improvement has been made during the last few years in laboratory measurements of reactivity of doubly-charged molecular ions and recombination with electrons, as reflected by the present special issue of PCCP. Very high resolution and high sensitivity instruments such as the Hubble Space Telescope or space-borne spectrometers open new possibilities to detect the predicted weak emissions of doubly-charged ions. *In situ* measurements by mass spectrometry can also be planned due to the improved mass resolution and sensitivity of instruments, and even possibly by a new generation of instruments which could distinguish ions with identical mass to charge ratio (m/q), as for N_2^{++} and N^+ for example. In these new conditions, it is now possible to pursue the study of this topic, which can lead to new insights into atmospheric processes, as doubly-charged ions are indicators of energetic processes, could play a significant role in atmospheric escape or induce new types of chemical reactions.

Let us mention that a huge and pioneering work on these peculiar ion species has been carried out since the late 1970s by S. V. Avakyan,[8,23,24,30–32] in particular on the following non-exhaustive list of topics: analysis of the behaviour and role of O^{++} in the Earth's atmosphere; effect of solar flares; compilation of all necessary photo-chemical rates and cross sections related to the sources and sinks of doubly-charged ions; excitation and emissions of ions.

The aim of this article is to present the status of our knowledge on doubly-charged ions, and to provide the relevant information regarding their study in the upper atmospheres. This article has been targeted for the following readers: the planetary scientist who is carrying out either data analysis and/or modelling; the engineer who is designing space instrumentation; the laboratory physicist or chemist who is willing to provide appropriate information. The outline is as follows: after reviewing the present status of positive detection of doubly-charged ions in planetary atmospheres, we provide a comprehensive review of their photochemistry. Afterwards, we discuss three possibilities to detect doubly-charged ions. Then we outline a few interesting implications of the formation of these ions in planetary atmospheres and summarize the work done in the field of numerical simulations of densities of doubly-charged ions in the ionospheres. Finally we give our view concerning next steps, challenges and needs for future work on this topic in the next 10–20 years.

2. Positive detection of doubly-charged ions in planetary ionospheres

Doubly-charged ions are minor ions in planetary ionospheres and their detection is rather difficult, as detailed in Section 3. These two reasons explain why this type of ions has not been detected in many atmospheres. To our knowledge, and at the time of writing, only atomic O^{++} ions have been measured in the ionospheres of Venus, Earth and Io, and the S^{++} ion in the ionosphere of Io.

For the Earth, several satellite measurements in the ionosphere have reported the detection of O^{++} ions by mass spectrometry.[3–6,11,15–17] Their density varies from 1 cm^{-3} at 160 km up to 100 cm^{-3} at 600 km altitude (see Fig. 1, from Fig. 1 of ref. 16). The data interpretation led to major findings concerning the source and loss processes of these ions (*e.g.*, ref. 33). The ion densities strongly vary with the geomagnetic activity (*e.g.* ref. 25, 34–36). Even though N_2^{++} and O_2^{++} are expected to exist in the Earth's atmosphere, they unfortunately cannot be distinguished from N^+ and O^+ signatures by mass spectrometry. Therefore, no direct detection of those species has been reported so far. It is worth mentioning that a very interesting study invokes the possible presence of auroral O_2^{++} ions in order to understand mass spectrometry data acquired during rocket experiments.[22] Though the authors stressed the exploratory nature of their study the derived ratio for O_2^{++}/O^+ is 0.12 at 140 km. Avakyan[30] suggested assigning some emission bands in the visible range to O_2^{++} and N_2^{++} ions. However this identification does not seem to be solid and will be discussed further in Section 3.

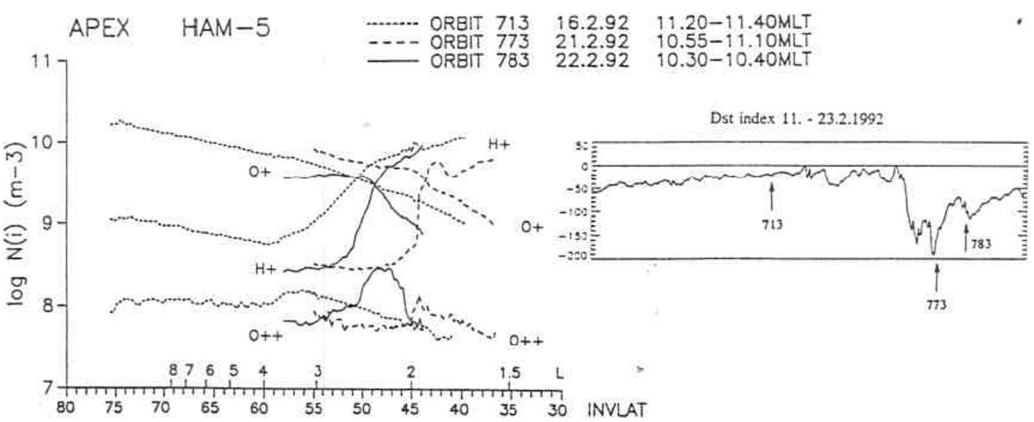

Fig. 1 Example of measurements of O^{++} in the Earth outer ionosphere (reprinted with permission from Truhlik.[16] Copyright 1997, Elsevier B.V.), together with other ions. The variation of densities is due to a geomagnetic storm. The O^{++} densities are enhanced by a factor of almost 10 in this particular period.

 This journal is © the Owner Societies 2011

View Article Online

Published on 19 September 2011. Downloaded by BELGIAN INSTITUTE FOR SPACE AERONOMY on 11/02/2016 11:00:19.

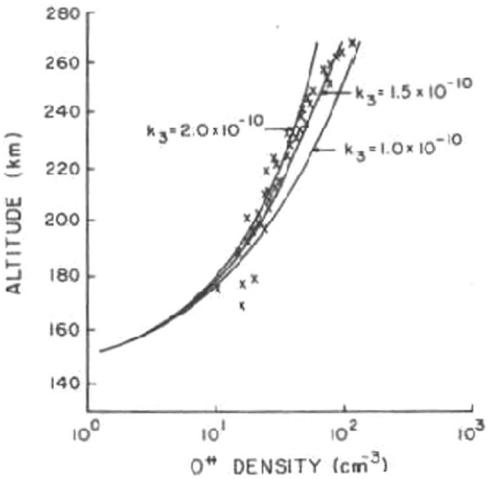

Fig. 2 Vertical profile of the O^{++} density in the atmosphere of Venus (from Fox and Victor,[37] copyright 1981 American Geophysical Union, reproduced by permission of American Geophysical Union). The measurements are represented with crosses. The solid lines display three models characterised by a different rate coefficient for the destruction of O^{++} by atomic oxygen.

In other planetary atmospheres, O^{++} ions have been detected in the ionosphere of Venus by the ion mass spectrometer on board the NASA Pioneer Venus Orbiter.[17,18] Densities reach typically 10 cm^{-3} at 170 km and 100 cm^{-3} at 280 km, on the dayside, as shown in Fig. 2. Model and observations are in relatively good agreement.[29,37] Peaks corresponding to a mass to charge ratio of 8, which could be a signature of O^{++} ions, are also detected in the Mars exosphere by Dubinin *et al.*[38] Molecular CO_2^{++} and N_2^{++} ions have been predicted to exist with significant densities in the Mars,[26,27] Venus[29] and Titan[28] ionospheres. This will be discussed in Section 5. Finally, in the Io's ionosphere, O^{++} and S^{++} ions have been identified with the NASA Galileo spacecraft plasma analyzers,[19,20] as well as the C^{++} and S^{++} ions by the far ultraviolet spectrometer FUSE instrument.[21] Its composition and dynamics are driven by the volcanic activity of the moon and by the interaction with the magnetosphere of Jupiter. Their typical density is 50 cm^{-3}. The O^{++} emissions at 70.3, 83.3 and 83.4 nm and the S^{++} emission at 68.5 nm were detected by the Voyager 1 and 2 UVS and the Cassini UVIS instruments.[39–42] The S^{++} emission at 953.1 nm was identified from the ground.[43] The Far Ultraviolet Spectroscopic Explorer detected a series of lines of S^{++} in the range of 101.2–112.8 nm,[21] as well as the C^{++} emission line at 97.7 nm.

Very recently, Linsky *et al.*[44] reported doubly charged atomic ions Si^{++} in the limb of the exoplanet HD 209458b. Some reduction of the Si^{++} emission line from the star at 120.65 nm, when transit occurs, suggests the presence of doubly charged species resulting from Si^{+} ionization by protons from the solar wind.

3.1 Doubly-charged ion facts: sources and sinks

We review here the basic understandings on the creation and loss processes of doubly-charged ions in a planetary ionosphere.

3.1.1 Production. A doubly-charged ion A^{++} or AB^{++} can be the result of one of the following six processes.

Double ionisation of neutral induced by photon or electron, Auger process, singly charged ion ionisation by photon or electron, and impact with high energy particles. Hereafter these processes are described and, when available, the quantitative information is summarized for the considered species.

For the sake of completeness, one should add another process that has been proposed in order to explain Titan blossoming chemistry, and involves molecular dication chemistry. Hence activation of methane, to release bigger dication after carbon–carbon coupling reactions, has been demonstrated for aromatic species.[45–48] This mechanism will be further described in Section 4.1 describing the exotic chemistry of molecular dications.

3.1.1.1 Double photoionisation of the neutral parent.

$$h\nu + A \rightarrow A^{++} + 2e$$

$$h\nu + AB \rightarrow AB^{++} + 2e$$

Table 1 gives the relevant ionisation thresholds.

When the threshold for double ionisation is unknown, we propose to use the empirical method recently refined by Molloy *et al.*[57] This method, based on examination of data for a wide range of molecules, leads to calculation of double ionisation energies from the molecule single ionisation energies and maximum molecular dimensions.

Table 2 gives the most recent source of information for the double photo-ionisation cross sections. Energy dependence of the cross sections for the production by photoionisation of molecular dications is also shown in Figures 3–5. In Tables 2 and 3, some cross section values are given and they are expressed in cm^2 (10^{-18}). Let us remind that 1×10^{-18} cm^2 is equal to 1 Megabarn (Mb).

The double photoionisation cross sections of N_2 have only very recently been measured experimentally[67] and detailed results are not yet published. In order to predict the N_2^{++} density that could be expected in the Earth,[25] Venus[29] or Titan[28] ionospheres, we have used an empirical method based on the observation of a proportionality between electron impact ionisation,[72] and photoionisation.[59] Hence, Samson[59] showed that the double-photoionisation cross section is proportional to the electron-impact ionisation of the monocation multiplied by the total photoabsorption of the neutral species.

Table 1 Single and double ionisation thresholds

Neutral	Single ionisation threshold/eV (from ref. 49)	Double ionisation threshold/eV	Uncertainty/eV	Ref.
C	11.260	35.643	<0.001	49
N	14.534	44.135	<0.001	49
O	13.618	48.739	<0.001	49
CH_4	12.61	34.4	0.2	50
		32.3[a]	0.1	51
CO	14.014	41.268	0.02	52
N_2	15.581	42.88	0.10	53
NO	9.264	38.46	0.01	54
O_2	12.070	36.13	0.02	55
Ar	15.759	43.3886	<0.001	49
CO_2	13.777	37.340	0.01	56

[a] See the text, Section 3.2.2.

View Article Online

Published on 19 September 2011. Downloaded by BELGIAN INSTITUTE FOR SPACE AERONOMY on 11/02/2016 11:00:19.

Table 2 Photoionisation cross sections. The values with the indication "metastable dication" relate to the apparently stable molecular dication measured in experiments, which corresponds to species stable for longer than a few microseconds

Process	Ref.	Cross section (10^{-18} cm^2)	Uncertainty on the cross section (%)
$C + h\nu \rightarrow C^{++} + 2e$	58 (theory)	0.1 (maximum at 60 eV)	
$N + h\nu \rightarrow N^{++} + 2e$	59–61	0.21 (maximum at 60 eV)	15
	62	0.02 (maximum at 120 eV)	
$N_2 + h\nu \rightarrow N^{++} + N + 2e$	63	0.2 (maximum at 500 eV)	
$O + h\nu \rightarrow O^{++} + 2e$	60 and 64	0.23 (maximum at 80 eV)	
$CH_4 + h\nu \rightarrow CH_4^{++} + 2e$	65	0.084 (maximum at 47 eV)	10
		0 (metastable dication)	
$O_2 + h\nu \rightarrow O_2^{++} + 2e$	—	—	—
$O_2 + h\nu \rightarrow O^{++} + O + 2e$	63	0.2 (maximum at 600 eV)	
$CO + h\nu \rightarrow CO^{++} + 2e$	66	0.85 (maximum at 60 eV)	20
		0.1 (metastable dication)	
$N_2 + h\nu \rightarrow N_2^{++} + 2e$	67	0.2 (metastable dication)	3
	29	0.18 (estimated metastable dication)	
$NO + h\nu \rightarrow NO^{++} + 2e$	68 and 69	1.15 (maximum at 50 eV)	20
		0.16 (metastable dication)	
$Ar + h\nu \rightarrow Ar^{++} + 2e$	61	0.22	
$CO_2 + h\nu \rightarrow CO_2^{++} + 2e$	70	(Relative)	10
	71	1.7 (maximum at 55 eV)	20
		0.14 (metastable dication)	

We proposed to use a proportionality constant of 0.133×10^{16} cm^{-2} in order to obtain the cross section.[29] The measured cross sections by Wehlitz[67] show that this estimation was excellent (1.8×10^{-17} cm^{-2} estimated, 2.0×10^{-17} cm^{-2} normalized measured value at 59 eV electron energy). It could eventually be used for O_2.

3.1.1.2 Electron impact double ionisation of the neutral parent.

$$e + A \rightarrow A^{++} + 3e$$

$$e + AB \rightarrow AB^{++} + 3e$$

Table 3 gives the most recent source of information for the electron impact double ionisation cross sections.

3.1.1.3 Auger process. An Auger process is *a priori* an efficient route to produce doubly charged species, because (1s) core electron ionization (CE) of species from the second row of the periodic table essentially results in ejection of a second or Auger electron (AE), instead of fluorescence, as observed for heavier species.[85] This two step process occurs with almost no change of the molecular structures, and is therefore considered to be vertical. A distribution of final dicationic states is produced. We estimated in Table 4 from the published material the relative abundance of stable *versus* dissociative dications that result from this process.

$$h\nu \text{ or } e + A \rightarrow A^{+} + CE \rightarrow A^{++} + AE + CE$$

$$h\nu \text{ or } e + AB \rightarrow AB^{+} + CE \rightarrow AB^{++} + AE + CE$$
$$\rightarrow A^{+} + B^{+} + AE + CE$$

3.1.1.4 Single photo-ionisation of the ion A^+ or AB^+. This process is generally of limited relevance in ionospheres as ionic species are already minor constituents, making this process

Table 3 Electron impact ionisation cross sections. The values with the indication "metastable dication" relate to the apparently stable molecular dication measured in experiments, which corresponds to species stable for longer than a few microseconds

Process	References	Cross section (10^{-18} cm^{-2})	Uncertainty on the cross section
$C + e \rightarrow C^{++} + 3e$	—	—	—
$N + e \rightarrow N^{++} + 3e$	—	—	—
$O + e \rightarrow O^{++} + 3e$	73 and 74	5.1 (max at 190 eV)	
$CH_4 + e \rightarrow$ fragment ions	75	5 (max at 125 eV)	±15% for $CH_2^+ + H^+$
	50		±20% for $C^+ + H^+$
$CO + e \rightarrow CO^{++} + 3e$	76	15 (max at 150 eV)	15%
		0.9 (metastable dication)	
	77	0.8 (metastable dication)	10%
$N_2 + e \rightarrow N_2^{++} + 3e$	78	14 (max at 150 eV)	10%
		1.5 (metastable dication)	
		1.6 (max at 160 eV)	
$N_2 + e \rightarrow N^{++} + 3e$	78		4%
$NO + e \rightarrow NO^{++} + 3e$	—	—	—
$O_2 + e \rightarrow O_2^{++} + 3e$	78–80	15 (max at 150 eV)	10%
		1.6[a] (metastable dication)	
$O_2 + e \rightarrow O^{++} + 3e$	78	2.25 (max at 225 eV)	5% up to 1000 eV
$Ar + e \rightarrow Ar^{++} + 3e$	81	19 (max at 95 eV)	4.5%
$CO_2 + e \rightarrow CO_2^{++} + 3e$	82	(Relative)	10%
	83	14.5 (max at 120 eV)	25%
		3.5 (metastable dication)	
	84	(Analytic compilation)	

[a] See the text, Section 3.2.6.

 This journal is © the Owner Societies 2011

View Article Online

Published on 19 September 2011. Downloaded by BELGIAN INSTITUTE FOR SPACE AERONOMY on 11/02/2016 11:00:19.

Table 4 Auger processes

Process	Core electron (1s) ionization energy/eV	Ref.	Comments
$C + e \rightarrow C^{++} + 3e$	291	86	
$N + e \rightarrow N^{++} + 3e$	404.8	86	
$O + e \rightarrow O^{++} + 3e$	538	86	
$CH_4 + e$ (5 keV)	293	87	Completely dissociative
$CO + h\nu \rightarrow C^{+} + O^{+} + 2e$	296, 542	88 (keV electron C1s and O1S)	Leads to dissociative states of the molecular dication
$N_2 + h\nu \rightarrow N^{+} + N^{+} + 2e$	410	89	More than 95% dissociative
$NO + h\nu \rightarrow N^{+} + O^{+} + 2e$	410, 544	90	Total KERD maximum at 10 eV
$NO + e \rightarrow N^{+} + O^{+} + 3e$	410, 544	91	More than 90% dissociative
$O_2 + h\nu \rightarrow O^{+} + O^{+} + 2e$	544	85 and 92	Totally dissociative
		93	Theoretical simulation
$O_2 + e \rightarrow O^{+} + O^{+} + 3e$	544	94	Totally dissociative
$CO_2 + h\nu \rightarrow O^{+} + CO^{+} + 2e$	297, 541	95 (photons C1S)	More than 60% dissociative the rest is metastable and furthermore no population of triplet ground state which is the only stable in the ionosphere
$CO_2 + e$ (1.5 keV) $\rightarrow O^{+} + CO^{+} + 3e$	297, 540	88 (keV electron C1s and O1S)	More than 90% dissociative the rest is metastable and furthermore no population of triplet ground state which is the only stable in the ionosphere

minor compared to neutral direct double ionisation described in previous tables. However, in the case of atomic ions, the limited rate of electronic recombination makes it a relevant process, specifically in outermost ionospheres.[25]

$$h\nu + A^{+} \rightarrow A^{++} + e$$

Table 5 gives the most recent source of information for the single ion photo-ionisation. Let us note that the measured cross sections for molecules are those to form the parent doubly-charged ions detected in the experimental set-ups, *i.e.* which have a lifetime longer than a few microseconds (*i.e.* the cross sections related to metastable dications in Tables 2–4). Molecular parent doubly-charged ions which quickly dissociate, faster than a few microseconds, are not included in the reported ionisation cross sections. The total ion photoionisation cross sections including fast dissociative channels could be an order of magnitude larger.

3.1.1.5 Electron impact second ionisation of the ion A^{+} or AB^{+}. As for photon impact second ionization of ions, this process is of limited relevance in ionospheres except in the case of atomic ions, especially in outermost ionospheres.[25]

$$e + A^{+} \rightarrow A^{++} + 2e$$

Table 6 gives the most recent source of information for the ion electron impact ionisation cross sections.

3.1.1.6 High energy particle bombardment. Protons of energies lower than 10 keV are not discussed here as only sparse theoretical and experimental data are available. For a review of available experimental data on the subject, see the study of Avakyan *et al.*[31] Table 7 gives information for the production of dications by high energy particle impact

3.1.2 Loss. A doubly-charged ion A^{++} or AB^{++} can be lost through one of the following reactions.

3.1.2.1 Chemical reaction with a neutral component.

$$A^{++} + M \rightarrow A^{+} + M^{+}$$

$$AB^{++} + M \rightarrow AB^{+} + M^{+}$$

$$AB^{++} + M \rightarrow A^{+} + BM^{+}$$

Reaction rate constants k for doubly-charged ions are reported in Table 8. Few experimental data are available, so we have also reported calculated or estimated rate constants. For some reactions, the authors have not measured reaction rate constants, but reaction cross sections as a function of collision energy in the centre of mass (CM) frame. We have reported these cross section values in $Å^2$, but they can be converted into rate constants, using the following formula

Table 5 Known cross sections for the photoionisation of ions

Process	Ref.	Threshold/eV	Cross section (10^{-18} cm^{-2})
$C^{+} + h\nu \rightarrow C^{++} + e$	96	24.383	4.1 at threshold 0.5 at 100 eV with resonances
	97		Theory
$N^{+} + h\nu \rightarrow N^{++} + e$	98	29.601	7 at threshold 1.1 at 80 eV with resonances
	97		Theory
$O^{+} + h\nu \rightarrow O^{++} + e$	99	35.121	10.6 at threshold 9.8 at 44.4 eV with resonances uncertainty 15 to 20%
$CO^{+} + h\nu \rightarrow CO^{++} + 1e$	100	27.3	2.5
	101		Theory
$N_2^{+} + h\nu \rightarrow N_2^{++} + 1e$	102	27.30	1
$NO^{+} + h\nu \rightarrow NO^{++} + 1e$	—	—	—
$O_2^{+} + h\nu \rightarrow O_2^{++} + 1e$	—	—	—
$Ar^{+} + h\nu \rightarrow Ar^{++} + 1e$	103	27.630	Theory
$CO_2^{+} + h\nu \rightarrow CO_2^{++} + 1e$	—	—	—

View Article Online

Published on 19 September 2011. Downloaded by BELGIAN INSTITUTE FOR SPACE AERONOMY on 11/02/2016 11:00:19.

Table 6 Cross sections for electron impact ionisation of ions

Reaction	References	Threshold/eV	Cross section (10^{-18} cm^{-2})	Uncertainty on cross section (%)
$C^+ + e \rightarrow C^{++} + 2e$	104	24.383		
$N^+ + e \rightarrow N^{++} + 2e$	104	29.601		
$O^+ + e \rightarrow O^{++} + 2e$	105	35.121	45.3 (max at 150 eV)	±10
$CO^+ + e \rightarrow CO^{++} + 2e$	106	27 ± 0.5	15 (metastable dication)	±15
	107		150 total	Theoretical model
$N_2^+ + e \rightarrow N_2^{++} + 2e$	72	27.9 ± 0.5	53 (max at 120 eV)	±5.7
$NO^+ + e \rightarrow NO^{++} + 2e$	—	—	—	—
$O_2^+ + e \rightarrow O_2^{++} + 2e$	108	24.0 ± 1	0.8 (max at 140 eV)	±20
	107		1.2 (max at 140 eV)	Theoretical model
$Ar^+ + e \rightarrow Ar^{++} + 2e$	109	27.630	117 (max at 78 eV)	±10
$CO_2^+ + e \rightarrow CO_2^{++} + 2e$	110	23.9 ± 0.5	50 (metastable dication)	±0.2
	107		200 total	Theoretical model

Table 7 Production of dications by high energy particle impact

Reaction	Ref.	Energy range	Cross section (10^{-18} cm^{-2})	Uncertainty on cross section (%)
$CO + H^+ \rightarrow CO^{++} + H^+ + 2e$	111	10–14 000 keV	100 stable	50
$CO_2 + e^- \rightarrow CO_2^{++} + 3e$	112	10–26 keV	0.25 stable	8

Table 8 Rate constants k or cross sections σ of reactions of doubly-charged ions

Reaction	k/cm^3 s^{-1}	σ/cm^2	Measurement energy	Ref.	Uncertainty on the value (%)
$C^{++} + H \rightarrow C^+ + H^+$		5.1×10^{-19}	2 eV u^{-1}	114	50
$C^{++} + He \rightarrow C^+ + He^+$		5.9×10^{-17}	2 eV u^{-1}	114	50
$N^{++} + He \rightarrow N^+ + He^+$	8.67×10^{-11}		0.6 eV CM	115	8
$N^{++} + H_2 \rightarrow$ products	3.38×10^{-11}		0.34 eV CM	116	10
$N^{++} + N_2 \rightarrow$ products	2.10×10^{-9}		1.8 eV CM	116	9
$N^{++} + CO \rightarrow$ products	3.37×10^{-9}		1.8 eV CM	116	9
$O^{++} + H \rightarrow O^+ + H^+$	1.1×10^{-9} (theory)		200 to 20 000 K	117	
$O^{++} + He \rightarrow O^+ + He^+$	1.12×10^{-12} for O^{++} ^3P			118	13
	1.0×10^{-9} for O^{++} ^1D			119	(Theory)
$O^{++} + O \rightarrow O^+ + O^+$	1.06×10^{-10}			25	40
$O^{++} + N_2 \rightarrow O^+ + N_2^+$	1.3×10^{-9}		300 K	120	25
	3.15×10^{-9}		2.5 eV CM	18	9
$O^{++} + O_2 \rightarrow O^+ + O_2^+$	1.5×10^{-9}		300 K	120	20
		3.5×10^{-15}	3 to 400 eV u^{-1}	121	10
$O^{++} + CO_2 \rightarrow$ products	2×10^{-9}			37	25
$O^{++} + CO \rightarrow$ products	3.40×10^{-9}		At 2.5 eV CM	118	9
$O^{++} + Ar \rightarrow O^+ + Ar^+$		2.0×10^{-15}	3 to 400 eV u^{-1}	121	10
$CO^{++} + He \rightarrow$ products		0.9×10^{-16}	49 eV	122	100
$CO^{++} + Ar \rightarrow CO^+ + Ar^+$		1×10^{-15}		122	60
$CO^{++} + Ar \rightarrow CO^{+*}$ (B state) $+ Ar^+$		1.9×10^{-18}		123	20
$CO^{++} + Ar \rightarrow ArC^{++} + O$		2×10^{-20}	2 eV CM	124	20
$CO^{++} + H_2 \rightarrow CO^+ + H_2^+$		σ not measured	4 keV	125	—
$CO^{++} + O_2 \rightarrow CO^+ + O_2^+$		σ not measured	4 keV	125	—
$N_2^{++} + O \rightarrow$ products	1.8×10^{-9}			29	55
$N_2^{++} + O_2 \rightarrow N_2^+ + O_2^+$	2.8×10^{-9}			25	25
$N_2^{++} + N_2 \rightarrow N_2^+ + N_2^+$	2.7×10^{-9}			28	25
$N_2^{++} + CO_2 \rightarrow$ products	3×10^{-9}			29	60
$O_2^{++} + N_2 \rightarrow O_2^+ + N_2^+$	2×10^{-9}			126	25
$O_2^{++} + O_2 \rightarrow O_2^+ + O_2^+$	2×10^{-9}			126 and 127	25
$O_2^{++} + NO \rightarrow O^+ + NO_2^+$	1.8×10^{-9}		0.04 eV	126	15
	1.3×10^{-9}		0.087 eV		20
$O_2^{++} + CO_2 \rightarrow O_2^+ + CO_2^+$	2.3×10^{-9}		0.04 eV	126	10
	2.7×10^{-9}		0.125 eV		10
$CO_2^{++} + O \rightarrow$ products	2×10^{-9}			29	60
$CO_2^{++} + CO_2 \rightarrow$ products	2.13×10^{-10} $(T_n/300)^{0.5}$			26	20
$CO_2^{++} + He \rightarrow$ products	Negligible			128	
$CO_2^{++} + Ar \rightarrow$ products		32.7×10^{-18}	49 eV	128	

$$k\ (\text{cm}^3\ \text{s}^{-1}) = \sigma\ (\text{cm}^2) \times \langle v\ (\text{cm s}^{-1})\rangle = \sigma\ (\text{Å}^2) \times 10^{-16} \times \langle v\ (\text{cm s}^{-1})\rangle$$

where k is the reaction rate constant, σ the reaction cross section and $\langle v\rangle$ the mean relative velocity *i.e.*

$$\langle v\ (\text{cm s}^{-1})\rangle = 9.82 \times 10^5 \sqrt{(2E\ (\text{eV})/\mu\ (\text{u})}$$

where E is the centre of mass collision energy in eV and μ the reduced mass of the collision partners in atomic mass units ($1/\mu = 1/m_1 + 1/m_2$ where m_1 and m_2 are the masses of the

 This journal is © the Owner Societies 2011

View Article Online

Published on 19 September 2011. Downloaded by BELGIAN INSTITUTE FOR SPACE AERONOMY on 11/02/2016 11:00:19.

two collision partners). At 300 K, E is approximately equal to 0.025 eV. Some cross section values are given in Megabarn (Mb) in the original papers (1 Mb = 10^{-18} cm^2). When a cross section has only been measured at collision energies larger than a few eV, it is not possible to extrapolate its value at 300 K, so we have chosen to report in Table 8 only the corresponding reaction cross sections σ at the measured CM collision energy and not the calculated rate constants k. Let us mention the very useful bibliographic plasma database GAPHYOR,[113] which is particularly relevant for ion reactions with a neutral atom or molecule, as well as for ion recombination reactions with electrons. This database covers collision energy ranges from thermal energies until energies greater than 10 keV.

Let us make a few remarks about the values reported in Table 8: Johnsen and Biondi[120] did not measure any difference between O^{++} ^3P ground state and O^{++} ^1D metastable state reactions with N_2 and O_2. The rate constant value of the $O^{++} + CO_2$ reaction cited by Fox and Victor[37] comes from measurements made by Johnsen and Biondi. Note that the products of the reaction between O_2^{++} and NO are surprising ($NO_2^+ + O^+$), as the charge transfer channel ($NO^+ + O_2^+$ products) is not observed.[126] Mathur and Rajgara[125] have studied the CO^{++} reaction with H_2, He, O_2 and Kr with a translational spectrometry technique at 4 keV energy. For the reaction with H_2 and O_2, they have not observed the dissociative charge transfer ($CO^+ + H^+ + H$ and $CO^+ + O^+ + O$), but only the $CO^+ + H_2^+$ and $CO^+ + O_2^+$ channels. These authors did not measure the reaction cross sections, but from the mechanism they observed, it can be reasonably assumed that these reactions are effective and their rate constant at 300 K is probably in the range of a few 10^{-9} cm^3 s^{-1}.

3.1.2.2 Recombination with a thermal electron.

$$AB^{++} + e \rightarrow A + B^+$$

$$AB^{++} + e \rightarrow A^+ + B$$

$$A^{++} + e \rightarrow A^+ + h\nu$$

Table 9 gives the recombination rate coefficient for a given dication.

Let us note that the electron recombination of doubly-charged atoms is only possible by radiative recombination in ionospheric conditions and that only calculated rate constants may exist. Kato and Asano[131] made a compilation of recombination rate coefficients calculated with empirical methods as a function of the electron energy. For C^{++}, N^{++} and O^{++} ions, the calculated rate constants have a maximum value of about 5×10^{-11} cm^3 s^{-1}.

3.1.2.3 Natural dissociation process. This process is restricted to molecular dications, and results from the generally encountered exothermicity of the dissociation into two singly charged fragments. Many small molecular dications present deep well that allow the species to survive this natural dissociation, but this is often limited to the lowermost electronic and vibrational states. The quasi-stable states will ultimately tunnel through the barrier and release fragments which will repel each other because of the Coulomb repulsion. This leads to kinetic energy release, which can be measured, and may be important in atmospheric processes such as escape.

$$AB^{++} \rightarrow A^+ + B^+$$

Let us note that molecular doubly-charged ions which are considered to be stable in laboratory experiments are those which have a lifetime longer than the detection time, which is typically of several microseconds. However in ionospheric conditions, stable doubly-charged ions must have a lifetime of at least 1 second, the typical time between collisions at altitudes corresponding to the peak ionic density of the ionosphere. One should therefore assess the different lifetimes of molecular dications (Table 10). This effect of population reduction is difficult to quantify in the absence of direct measurements.

3.2 Review of the individual ions

3.2.1 C^{++}, N^{++} and O^{++}. The double ionisation potential of C, N and O atoms is well known and has been determined with a high precision of better than 0.001 eV.[49] Already in 1941, Hagstrum and Tate[138] observed the formation of N^{++} and O^{++} doubly charged atomic ions in the dissociative ionisation by electron impact of N_2 and O_2, respectively. The double photoionisation cross sections have been measured experimentally for N and O,[59,61,64] but not for C atoms, which are more difficult to produce in laboratory. By photoionisation, the ratio of doubly charged to singly charged ions has been calculated to be 6.6% at 60 eV photon energy for C atoms,[58] and measured to be 6.6% at 60 eV photon energy for N (ref. 59) and 10% at 80 eV photon energy for O atoms.[64] However only the double ionisation of O atoms by electron impact has been measured.[74] Ionisation of C^+, N^+ and O^+,

Table 9 Recombination reactions of doubly-charged ions

Reaction	α/cm^3 s^{-1}	Ref.	Uncertainty on the recombination coefficient (%)
$C^{++} + e \rightarrow C^+ + h\nu$	4.24×10^{-11} at 100 K	97	10 to 20 calc.
$N^{++} + e \rightarrow N^+ + h\nu$	4.18×10^{-11} at 100 K	97	10 to 20 calc.
$O^{++} + e \rightarrow O^+ + h\nu$	$2.1 \times 10^{-11} \times 4/(1/2\,(T_e + T_i))^{0.5}$	129	Theory
$O_2^{++} + e \rightarrow$ products	—	—	—
$CO^{++} + e \rightarrow C + O^+ \rightarrow C^+ + O$	3.0×10^{-7}	130	50
$N_2^{++} + e \rightarrow$ products	$5.8 \times 10^{-7}\,(300/T_e)^{0.5}$	130	25
$NO^{++} + e \rightarrow$ products	—	—	—
$Ar^{++} + e \rightarrow Ar^+ + h\nu$	$\sim 3 \times 10^{-11}$ at T_e 10 eV	131	Theory
$CO_2^{++} + e \rightarrow$ products	$6.2 \times 10^{-7}\,(300/T_e)^{0.5}$	132	30

View Article Online

Published on 19 September 2011. Downloaded by BELGIAN INSTITUTE FOR SPACE AERONOMY on 11/02/2016 11:00:19.

Table 10 Lifetime of the doubly charged ions. The values correspond to experimentally measured quantities, except for theoretical estimates explicitly stated. Values in the microsecond range derive from mass spectrometry, values in the second range derive from decay rates in storage rings

Ion	Lifetime	Ref.
CH_4^{++}	<100 ns	133
CO^{++}	4 s and 8 s	134
		135 (theory)
N_2^{++}	3 s for ground state	134
	μs for metastable excited states	53
NO^{++}	≫10 μs for ground state up to v = 12 (theoretical)	136
O_2^{++}	≫ms for ground state	137
CO_2^{++}	4 s for ground state	134
	μs for metastable excited states	56

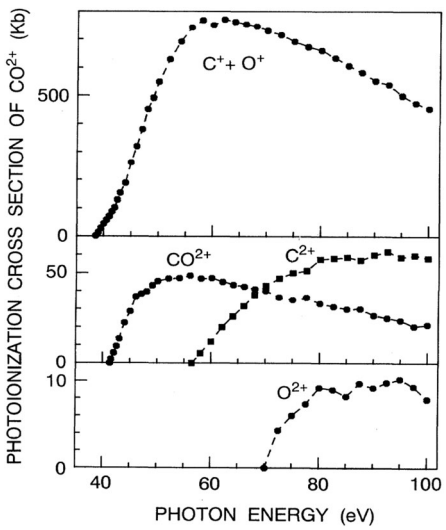

Fig. 3 Cross sections expressed in Kbarn (10^{-21} cm^2) for the production of CO^{++} by photoionisation of CO. Reproduced from Masuoka and Nakamura[66] by permission of the American Physical Society, copyright 1993 APS.

easier to prepare than the neutrals, has been measured both by photon and electron impact. For further information, the compilation of ionisation of atoms by electron impact made by Tawara and Kato[104] is very useful, as well as the review by Kjeldsen[139] on experimental ionisation cross sections of neutral atoms and atomic ions. Let us note that for the recombination reactions of atomic doubly charged ions, which can only be radiative recombination processes, there exist only theoretical calculations (see the review report by Kato and Asano[131]), due to the difficulty to measure experimentally such processes.

3.2.2 CH_4^{++}. Stable CH_4^{++} ions have never been observed. The doubly-charged molecular ion dissociates in less than 100 ns.[133] A recent study[50] showed that CH_4^{++} is formed in the same dissociative electronic states (ground $^3T_1$ and first excited $^1E_1$ states) when formed by 55 eV electrons or by 40.8 eV photons.[140] The $^3T_1$ state dissociates into $CH_3^+ + H^+$ and the $^1E_1$ excited state into $CH_2^+ + H^+ + H$ and $CH^+ + H^+ + H_2$. At this electron energy, these authors also observed the

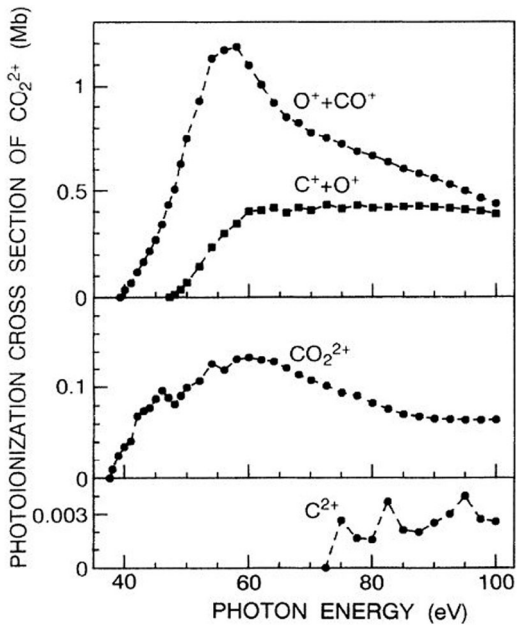

Fig. 4 Cross sections expressed in Mbarn (10^{-18} cm^2) for the production of CO_2^{++} by photoionisation of CO_2. Reproduced from Masuoka[71] by permission of the American Physical Society, copyright 1994 APS.

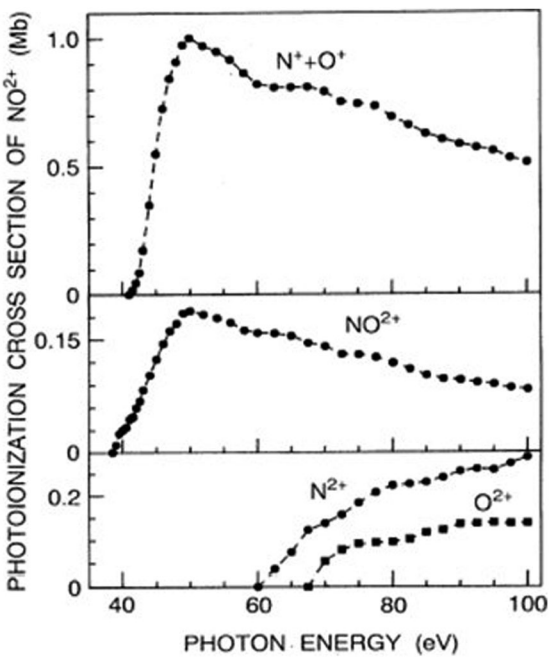

Fig. 5 Cross sections expressed in Mbarn (10^{-18} cm^2) for the production of NO^{++} by photoionisation of NO. Reproduced from Masuoka[69] by permission of the American Physical Society, copyright 1993 APS.

population of the first excited triplet state of CH_4^{++} ($^3T_2$) which dissociates into $CH_2^+ + H^+ + H$ and $CH^+ + H^+ + H_2$.

The adiabatic ionisation potential of CH_4^+ has been experimentally measured by a technique of charge stripping with molecular O_2 and calculated by an *ab initio* method to give a value of 19.7 eV.[51] The vertical ionisation potential of

 This journal is © the Owner Societies 2011

View Article Online

Published on 19 September 2011. Downloaded by BELGIAN INSTITUTE FOR SPACE AERONOMY on 11/02/2016 11:00:19.

CH_4 has been calculated to be 21.8 eV, according to the same authors.[51] This gives an adiabatic double ionisation potential of CH_4 of 32.3 eV, which is much lower than the measured appearance energy of 34.4 eV for dissociative double ionisation ion products reported by Ward *et al.*[50] This is due to the fact that the calculated planar geometry of CH_4^{++} is very different from the tetrahedral geometry of neutral CH_4.[141] By double photoionisation or electron impact ionisation, it is thus expected to observe the vertical double ionisation onset calculated to be equal to 34.4 eV, taking into account the difficulty to measure dissociation products of CH_4^{++} at threshold. However for photoionisation or electron impact ionisation of CH_4^{+}, for which there are no experimental values, it is expected to obtain values closer to the adiabatic one, as CH_4^{+} is planar.[51] This is the reason why we put two different values of ionisation thresholds in Table 1.

3.2.3 CO^{++}. CO^{++} was the first multiply-charged molecular species to be positively observed by mass spectrometry by Conrad in 1930.[142] Its double ionisation potential was already reported in 1931 with remarkable precision at 43 ± 1 eV,[143] to compare to the current best estimate of 41.268 ± 0.02 eV.[52] Though it exhibits very long-lived states (reported up to 8 s by Mathur *et al.*[134]) it has not been studied nor modelled in planetary ionospheres, CO being a minor species of planetary atmospheres. Hence evidence of the CO^{++} dication has never been reported, and would anyhow be particularly difficult. The first reason is the overlap of its signature in mass spectrometry with N^+ ions, the second is the absence of a clear signature in emission.[144]

Tables 1–10 summarise processes encountered in planetary ionospheres. Let us recommend recent works which provide useful information for ionospheric studies. Concerning spectroscopy and molecular dynamics, CO^{++} is particularly attractive to experimentalists developing new instruments or theoretical methods and it is used as a benchmark. The latest theoretical work on CO^{++} is by B. Mondal *et al.*,[145] revisiting the detailed experimental and theoretical work performed by Eland *et al.*[52] Kinetic energy release (KER) by dissociation of the dication after photoionisation was studied by Hsieh and Eland,[146] with KER values up to 11 eV at a photon energy of 48.4 eV and after electron impact by Lundqvist *et al.*,[147] with KER up to 22 eV at 200 eV electron energy. Lifetime measurements were performed in the nanosecond time range by Bouhnik *et al.*[148] and calculated by Sedivcova *et al.*[149] and Mrugala (Fig. 6).[135]

Regarding the reactivity, surprisingly, though CO^{++} reactivity with rare gases was very early studied,[150] very few studies have been reported later on. In atmospheres, the most relevant reaction that was studied is that with argon. Beyond the cross section and products,[122] this reaction was further described in terms of minor channels leading either to $CO^{+}*$ (B to X fluorescence),[123] or to the intriguing reaction product ArC^{++}.[124]

Emissions from CO^{++} were tentatively reported by Cossart and Robbe,[144] but this work has not been confirmed since and was even recently doubted by Mrugala.[135] As sensitivity and resolution of instruments is permanently improving, it would be good to have a definitive confirmation of these or other emissions from the dication. Reactivity is also an issue and it is important to perform experimental studies of the CO^{++} reaction with O_2, as these two species may coexist in planetary atmospheres.

3.2.4 N_2^{++}. Thomson[151] was the first to report on the possible presence of N_2^{++} in early mass spectrometry studies, but the result was questioned as molecular dications were considered at that time to be unstable species, driven by Coulomb repulsion. In 1941, Hagstrum and Tate[138] unequivocally identified a stable state of N_2^{++}. This was the beginning

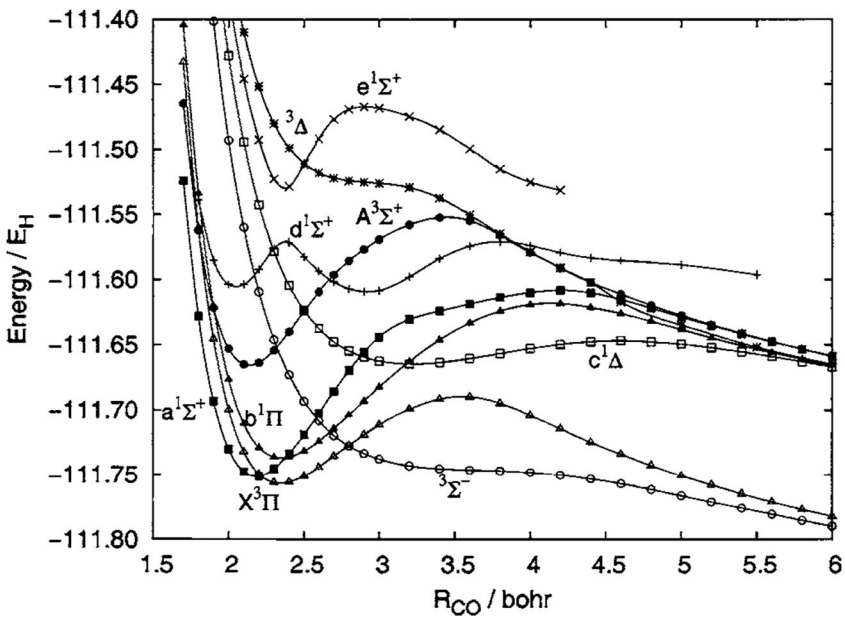

Fig. 6 Potential energy curves of the CO^{++} electronic states, reprinted with permission from Sedivcova *et al.*[149] Copyright 2006, American Institute of Physics. Energy is reported in Hartree, let us remind the conversion factor 1 Hartree = 27.211 eV.

View Article Online

Published on 19 September 2011. Downloaded by BELGIAN INSTITUTE FOR SPACE AERONOMY on 11/02/2016 11:00:19.

of a long history of experimental and theoretical exploration of the structure and reactivity of N_2^{++} ions, which constitutes an impressive set of information that can be confidently used to model the abundance and effects of such species in planetary ionospheres.

The double ionisation threshold of molecular nitrogen, together with the spectroscopy of the states located up to 11 eV above threshold have been measured very accurately by Ahmad *et al.*[53] using coincidence methods. The value of 42.88 ± 0.01 eV is found to be in excellent agreement with previous experimental[152,153] and theoretical[154] works (Fig. 7). Ahmad *et al.*[53] showed that the double ionisation at threshold is non-dissociative and becomes dissociative in the micro second time range above 44.5 eV, producing $N^+ + N^+$ fragments.

For double ionisation cross sections, it is important to distinguish between the cross section of double ionisation and the cross section of stable dication production. The first term corresponds to a direct or indirect mechanism, such as an Auger process, and it will often lead to a fast dissociation of the molecule into $N^+ + N^+$. The second process is unequivocally revealing the double ionisation, but is much less probable, as few states of the dication are non-dissociative. The contribution of multiple ionisation processes to the total ionisation is about 4% above 80 eV photon energy.[67]

Singly-charged ions coming from the fast dissociation of multiply-charged parent ions can only be distinguished from fragments coming from singly charged ions by the fact that they are produced in pairs. To our knowledge, for electron impact ionisation, only one study has been performed to quantify the relative intensity of ion pair production to total ion production. It is the work of Brehm and Defrenes,[155] who estimated the ratio at 3% at 1000 eV, and 5% at 150 eV. Absolute cross section measurements of N_2^{++} production are not easy, due to the mass-to-charge overlap with the N^+ fragment. This is the reason why many studies limit their absolute cross section information to a quoted 'N^+ and N_2^{++}' channel corresponding to ions having a mass-to-charge ratio of 14.[78,79,156] However, Märk[80] performed a study using a mass spectrometer with sufficient mass resolution and sensitivity in order to detect accurately the $^{14}N^{15}N$ dication (m/q = 14.5). Märk gives absolute cross sections for electron impact double ionisation from threshold up to 170 eV electron energy. The maximum cross section is 1.3×10^{-18} cm^2 ± 5% and corresponds to an electron energy of 125 eV. This result is in very good agreement with the previous result of Halas and Adamczyk[157] which extends to 600 eV, but has been criticised by Straub *et al.*[79] and later on by Tian and Vidal.[78] The latter showed that the measurements by Märk were probably underestimated by 20%.

Mathur *et al.*[134] have shown that N_2^{++} has no or very few states with lifetime in the range of micro to milliseconds. We propose to consider that values of the absolute cross section recorded in the microsecond time range are still valid in the ionospheric time range (see Section 4.2 for further discussion of dication lifetime).

Though the density of ions in ionospheres is insufficient to consider the competitive production of molecular dications by single ionisation of ions, let us mention that data exist for electron impact ionisation of N_2^+, which has been recorded by Bahati *et al.*[72] To our knowledge, there is only a very recent, not yet published, work[102] for the equivalent process induced by photons.

The metastable lifetime of N_2^{++} towards its dissociation into $N^+ + N^+$ has been determined by Mathur *et al.*[134] by monitoring their decay curves in a heavy-ion storage ring. The longest lifetime component is measured in the range of 3 seconds. They performed *ab initio* configuration interaction calculations of the potential energy curve for the lowest-energy state of N_2^{++} in order to compute tunnelling times of each vibrational level. They find that lifetimes in the range of 3 seconds would correspond to v = 10 of the ground state, and therefore propose to associate the experimentally measured lifetime to the effect of interactions with the residual gas in the ring, and consider that a lifetime of v = 0 is infinite. Another experimental evidence of the long lifetime of lower excited states is provided by Ahmad *et al.*[53] showing that a stable dication signature is still visible in the coincident mass spectra at v = 7 of the dication ground state. Many excited electronic states have been calculated and observed experimentally (see ref. 53 and 158 and references therein).

Due to the Coulomb repulsion, the charge separation is releasing a large quantity of kinetic energy, shared equally between the two N^+ fragments. The kinetic energy release in the dissociation has been measured by Brehm and Defrenes[155] for electron impact, and by Besnard *et al.*[159] for photoionisation. The kinetic energy release distribution can be described by a broad Gaussian curve, centred at 9 eV, with 6 eV FWHM. Thermodynamically, Besnard *et al.*[159] showed that the dissociation leads systematically to the atomic ions in their ground state, which puts a lower limit of 4.8 eV on the kinetic energy release. Using Doppler-free kinetic energy spectroscopy and an electron energy of 200 eV, Lundqvist *et al.*[158] recorded a KER spectrum that exhibits a high energy tail going up to 30 eV. N_2 dications can eventually dissociate by loss of a neutral N fragment, to produce N^{++}. The photoinduced process was studied by Franceschi *et al.*[62] They show that the dication asymmetric dissociation has a threshold at 59.9 ± 0.2 eV, and exhibits a maximum cross section of 2×10^{-20} cm^2 at 85 eV. Crowe and McConkey[160] measured the cross section for electron impact and showed that it is peaking around 190–195 eV, with a cross section of 1.9×10^{-18} cm^2.

Very few molecular dications are known to fluoresce. In the case of N_2^{++}, only the $D^1\Sigma_u^+$ (v = 0) → $X^1\Sigma_g^+$ (v = 0) transition has been identified[161,162] (see Section 3). The cross section for the photo-production of this emission has been determined by Ehresmann *et al.*[163] in the energy range from threshold at 51 eV to 66 eV, where it peaks at a value of 1×10^{-20} cm^2. This quantitative information was used to predict the stable N_2^{++} ion density that could be detected in the Earth,[25] Venus[29] or Titan[28] ionospheres.

Single charge transfer is the dominant product channel for chemical reactions of N_2^{++} ions with Ar, N_2 and O_2 (unpublished work from the authors R. Thissen and O. Dutuit). This charge transfer is mainly non-dissociative, but dissociative charge transfer has also been observed, as well as weak channels involving a chemical reaction, such as the formation of NO^+ ions in the $N_2^{++} + O_2$ reaction.[164] Absolute cross sections for the electron dissociative recombination have been measured

 This journal is © the Owner Societies 2011

View Article Online

Published on 19 September 2011. Downloaded by BELGIAN INSTITUTE FOR SPACE AERONOMY on 11/02/2016 11:00:19.

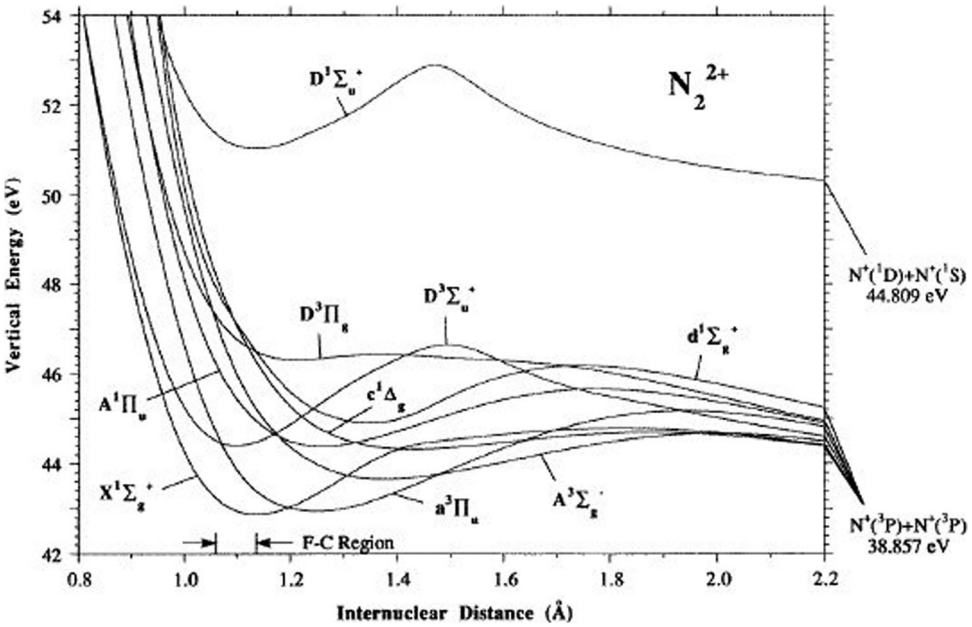

Fig. 7 Potential energy curves of N_2^{++} electronic states, reprinted with permission from Lundqvist *et al.*[158] Copyright 1996, IOP Publishing Ltd. The Franck Condon region from the neutral ground state is located between 1.06 and 1.13 Å.

by Seiersen *et al.*[130] using the heavy-ion storage ring ASTRID in the relative collision energy range 10^{-4}–10 eV. They measured a reaction rate constant about 2.5 times greater than the dissociative recombination of N_2^+ at room temperature. Beyond 10.9 eV collision energy, the asymmetric dissociation into N^{++} + N seems to be the dominant process. According to these authors, electron-collision-induced dissociation without electron capture is negligible.

3.2.5 NO^{++}. Because the molecular dication has no overlap with atomic fragments in the mass spectrum recorded by electron ionisation of NO, NO^{++} was identified and reported as soon as 1935 by Tate *et al.*,[165] and even a threshold of double ionisation was given (44 eV), in relatively good agreement with present values (38.46 eV[54]).

The spectroscopy of the molecular dication has been thoroughly studied (ref. 166 and references therein), and calculated (see ref. 136 and references therein). Three quasibound states exhibit vibrational series in the 5 eV above threshold. The Auger spectra were reported by Svensson and Karlsson.[91] The Auger process from both N and O 1s core levels leads essentially to dissociative states (we estimate more than 90% dissociation) and within the non-dissociative states, the first excited state is by far the most populated.

Undispersed fluorescence (~700 nm) has been detected from the first excited state by Besnard *et al.*[159] but as it is most probably distributed over a wide spectral range, no dispersed spectrum has been recorded yet. The transition from the second excited state was reported by Besnard *et al.*[167] and leads to the measurement of what is to date the highest resolution (rotational resolution) emission spectrum of a molecular dication by Cossart *et al.*[168,169] The search for the infrared spectrum of the NO^{++} dication has attracted a lot of interest since then, but has not yet been successful.[166,170]

Surprisingly however, this molecular dication has received limited interest in terms of measurements of the absolute cross section related to the production processes in the ionospheres. Hence, only its photoionisation cross section was measured by Samson *et al.*[68] and Masuoka.[69] The total (dissociative and non-dissociative) photo double ionisation cross section reaches 1.2×10^{-18} cm^2 at 50 eV (*i.e.* 13% of total ionisation cross section) while the cross section to produce molecular dication with lifetime beyond microsecond is at most 1.6×10^{-19} cm^2.

The absolute cross section for dication production by electron impact has not been reported to our knowledge, neither the ion ionisation into dicationic species. Let us mention that this information is of particular interest for NO, as this species is expected to be abundant as an ion in the upper atmospheres containing N and O (such as the Earth, or Venus).

The lifetime of NO^{++} has not been measured experimentally, but is expected to be very long (time scale reaching the second) according to the calculations by Bakova *et al.*[136]

The kinetic energy released distribution was measured by Hsieh and Eland,[146] and confirms results obtained at lower resolution in the energy range from 42 to 100 eV by Masuoka *et al.*,[171] with a released kinetic energy distribution presenting a maximum at 5 eV at threshold and increasing towards a plateau at 9 eV around 60 eV. This most probable KERD of 9 eV is observed as well at 400 and 540 eV by Suzuki and Saito[90] with the addition of a high energy tail up to 20 eV.

The electron dissociative recombination of NO^{++} has not been reported, nor calculated. The reactivity of NO^{++} was limited to experimental studies of collisions (keV regime) with noble gases.[172,173] It was shown to lead essentially (by a factor 10) to non-dissociative charge transfer, neither rate constant nor cross section measurements were performed.

View Article Online

Published on 19 September 2011. Downloaded by BELGIAN INSTITUTE FOR SPACE AERONOMY on 11/02/2016 11:00:19.

3.2.6 O_2^{++}. O_2^{++} was mentioned for the first time in 1941 by Hagstrum and Tate.[138] The O_2^{++} dication is very particular as the internuclear distance of its ground electronic state is amongst the shortest for diatomic systems (1.05 Å). This unexpected behaviour results from the removal of the two outermost unpaired electrons from neutral O_2, giving a particularly stabilized electronic structure.[174] Because of this important change in the equilibrium geometry between neutral and dicationic ground state, the direct ionization has tendency to populate a broad distribution of vibrational states.

The double ionization threshold was determined by Hall *et al.* in 1992[55] at 36.13 ± 0.02 eV, associated with an extended vibrational progression (up to $v = 20$). Spectroscopy of excited electronic states was studied by Eland,[54] in very good agreement with calculations performed by Edvardsson[137] from which we extracted the potential energy surfaces shown in Fig. 8.

The cross section for photo double ionization has not been measured and the electron impact double ionization was measured by Tian and Vidal[78] and Straub *et al.*[79] only as a combination of O^+ and O_2^{++} yields. Based on the assumptions of Märk[80] that O_2^{++} yield is less than 1% of O_2^+, one can estimate a maximum cross section of 1.6×10^{-18} cm^2 for the electron double ionisation process.

The Auger process has been studied in O_2, after photon[92] or electron[94] ionization of the O 1s core electron (540 eV). It yields final dissociative states of the dication. The process was simulated in detail by Bao *et al.*[93]

The molecular ion photoionisation was not reported. The equivalent process induced by electron was reported by Cherkani-Hassani *et al.*,[108] who found a maximum of 8×10^{-19} cm^2 cross section at 140 eV electron energy, in fairly good agreement with the predictions from the Deutsch Märk theory[107] at 1.2×10^{-18} cm^2.

The reactivity of O_2^{++} was evaluated in a drift tube instrument by Chatterjee and Johnsen[126] at thermal collision energy. Reaction rates with N_2, O_2, NO and CO_2 were measured to be in the 2×10^{-9} cm^3 s^{-1} range and lead to charge transfer, except in the case of NO, leading to NO_2^+ ion.

The dissociative recombination has not been reported, nor has the maximum lifetime of the molecular dication. Based on the calculations by Edvardsson,[137] it is however clear that the tunnelling is the only process leading to lower vibrational states of the molecular dication and it should probably lead to lifetimes in the range of seconds.

Kinetic energy release (KER) by dissociation of the molecular dication after photoionisation was studied by Hsieh and Eland,[146] with KER values up to 16 eV at a photon energy of 48.4 eV (broad Gaussian centred at 9 eV with 5 eV FWHM) and after electron impact by Lundqvist *et al.*,[175] with KER up to 22 eV at 200 eV electron energy.

For O_2^{++}, no emission has been identified so far. Avakyan[30] reports the possible identification of auroral emissions around 243 nm which he assigns to the $A^3\Sigma^+$–$B^3\Pi g$ transition. Three emission wavelengths have been tabulated by Avakyan[31] (see Table 12), based on previous calculated energies of O_2^{++} states.[176,177] These assignments were later on reassigned to emission lines from O^+ and O by Mahalingam and Hanson.[178] The fluorescence of O_2^{++} obviously needs further spectroscopy studies.

The missing information for this important molecular dication is obviously the photo double ionization of neutral and photoionisation of ion cross sections, together with clear characterisation of the metastable lifetime of the ground state in its various vibrational states.

3.2.7 Ar^{++}. Similar comments than for C^{++}, N^{++} and O^{++} atomic ions can be made for Ar^{++} ions, even though ionisation cross sections are much easier to measure than for radical atoms. Let us note that the ratio of doubly charged to

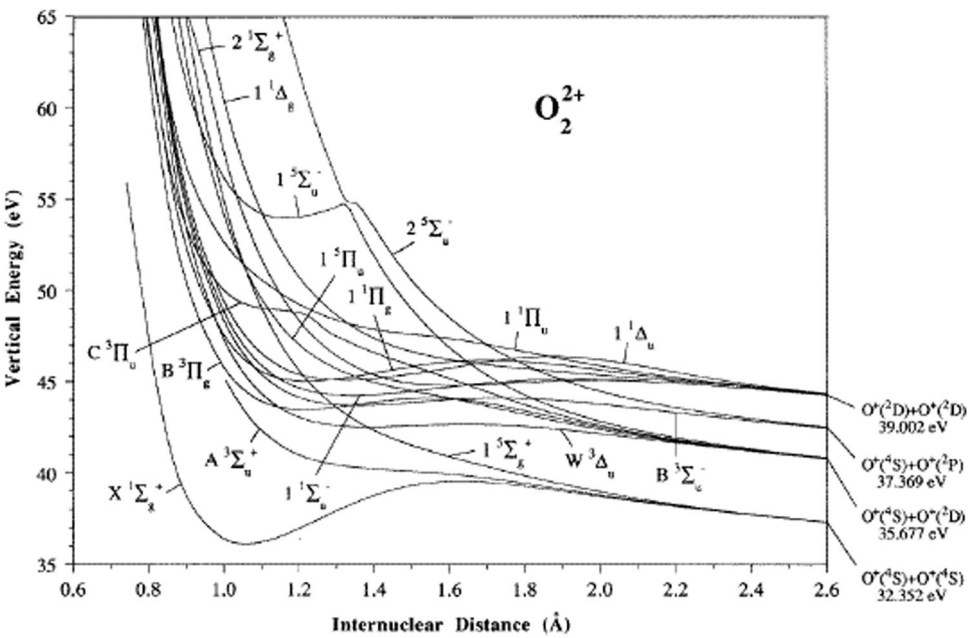

Fig. 8 Potential energy curves of the O_2^{++} electronic states, reprinted with permission from Lundqvist *et al.*[175] Copyright 1996, IOP Publishing Ltd. The Franck-Condon region from neutral ground state is located between 1.18 and 1.26 Å.

 This journal is © the Owner Societies 2011

View Article Online

Published on 19 September 2011. Downloaded by BELGIAN INSTITUTE FOR SPACE AERONOMY on 11/02/2016 11:00:19.

singly charged ions produced by ionisation reaches a value up to 19% from Ar^{++} threshold.[179] Even though it would not be so difficult to do, to our knowledge, the ionisation cross section of Ar^{+} has never been measured experimentally.

3.2.8 CO_2^{++}. First observed in a laboratory experiment in 1961,[180] CO_2^{++} is a good candidate for *in situ* detection by mass spectrometry as it would appear at $m/q = 22$, where the only interference would be the faint natural isotope of neon. It has attracted particular interest since the prediction of its abundance in the Mars atmosphere by Witasse *et al.*[26] This work predicted peak densities between 3 and 5 cm^{-3}. Let us note that a correction was published the next year by the same authors with slightly lowered values of 1.4 and 4.5 cm^{-3}.[27] This work was possible because of the existence of quantitative information for the main processes leading to production or loss of the molecular dication in the upper atmosphere. The method was refined by addition of new reaction rates and applied to the Venusian diurnal ionosphere by Gronoff *et al.*[29] leading to a predicted CO_2^{++} peak density in the Venus ionosphere of 30 cm^{-3} at 140 km altitude.

Tables 1–10 summarise quantitative information and relevant references at the time of writing for the production and loss processes encountered in planetary ionospheres.

Let us recommend further the recent works which provide useful information for ionospheric studies. Concerning spectroscopy and molecular dynamics, Sharma *et al.*[181] revisited the dication molecular dynamics and lifetimes, providing new insights on the metastable dissociation. This work based on experiments relying on electron ionisation parallels that of Slattery *et al.*,[56] who studied in great detail the photoionisation spectroscopy, together with the metastable dissociation, and confirmed the theoretical work of Hochlaf *et al.*,[182] predicting doubly-charged ion states and potential energy surfaces in the first 8 eV above threshold (Fig. 9). Alagia *et al.*[183] have done a detailed study of the kinetic energy released after dissociative photoionisation, and Püttner *et al.*[95] and Feyer *et al.*[88] both provided high resolution Auger spectra after either photo or electron excitation, respectively. Both works showed that the process leads either to direct dissociation of the dication or to a minor amount of excited doubly-charged ion states which are metastable in the microsecond time range. We therefore consider that in the ionospheric environment, the Auger process leads exclusively to dissociative double ionisation.

Concerning the reactivity of CO_2^{++} ions, early work consisted in studying the CO_2^{++} reactivity with rare gases.[128] The reaction products essentially come from dissociative charge transfer and their yield could be explained using the Landau–Zener theory. Franceschi *et al.*[184] have studied the reactivity with CO and CO_2. Beyond internal energy effects, they show a minor but unexpected O_2^{+} chemical product for both reactions and a specific dissociation of the dication in the homologous charge transfer with CO_2. This work triggered new experimental studies by Ricketts *et al.*,[46] Parkes *et al.*,[127] and Zabka *et al.*[185] The latter work, together with Roithova *et al.*[186] describes a very minor but intriguing mechanism leading to dicationic products according to $CO_2^{++} + CO_2 \rightarrow C_2O_3^{++} + O$, a further proof of exotic chemistry following dication reactivity, to be further discussed in Section 4.

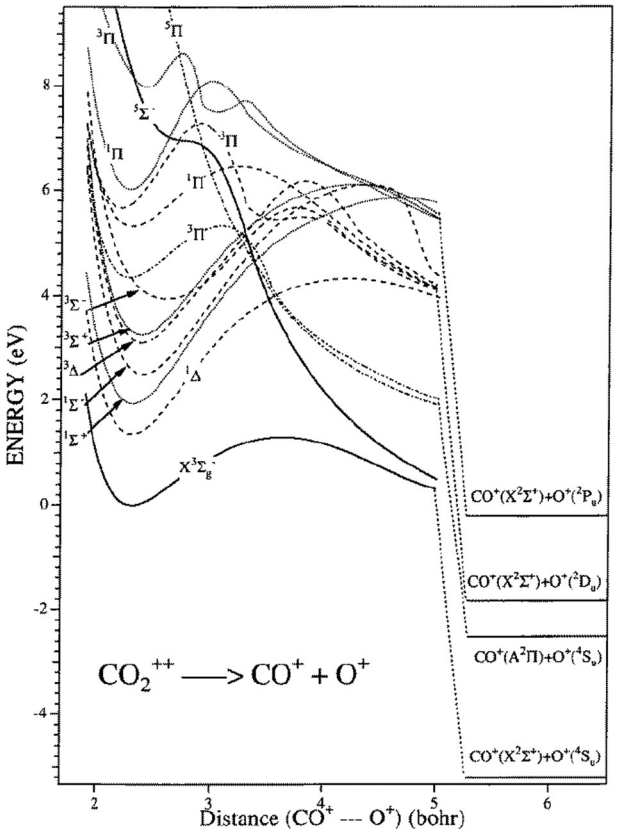

Fig. 9 CO_2^{++} potential energy surfaces, reprinted with permission from Hochlaf *et al.*[182] Copyright 1998, IOP Publishing Ltd.

Particularly missing information is the potential IR emissions that could help in remote detection of this dication in the dayglow of Mars or Venus, as well as absolute reaction cross sections for collisions with N_2 or O species present in Mars and Venus ionospheres.

4. Detectability of doubly-charged ions

4.1 Mass spectrometry

The first method to detect doubly-charged ions is by mass spectrometry, which allows measuring the mass-to-charge ratio for a given ion. Table 11 lists key values for the doubly-charged ions discussed in this review.

Doubly-charged ions can in principle be relatively easy to detect, as long as there is no overlap with other species which have the same mass-to-charge ratio (for example CO^{++} and N_2^{++}, both overlapping with N^{+}, or O_2^{++} overlapping with O^{+}). This detection obviously depends on the performances of the instrument: sensitivity and mass resolution are the important parameters to consider. With high-resolution mass spectrometry, it is possible to distinguish CO^{++} from N_2^{++} for example, using the fact that the nuclear mass defect is different for the two molecules (m/q is equal to 13.9969 and 14.0025 for CO^{++} and N_2^{++}, respectively). This separation requires a resolving power better than 3000. Up to now, only the Rosina/DFMS instrument on board Rosetta has a sufficient resolution to make those distinctions[187] but has not yet been in contact with

View Article Online

Published on 19 September 2011. Downloaded by BELGIAN INSTITUTE FOR SPACE AERONOMY on 11/02/2016 11:00:19.

Table 11 Mass to charge ratio and key values related to mass detection for doubly-charged ions discussed in this review

Ion	C^{++}	N^{++}	O^{++}	CO^{++}	N_2^{++}	NO^{++}	O_2^{++}	Ar^{++}	CO_2^{++}
m/q	6	7	8	14	14	15	16	20	22
m/q of second most abundant isotope peak	6.5	7.5	8.5	14.5	14.5	15.5	16.5	18	22.5
Relative abundance of second most abundant isotope peak[a]	1.1%	0.37%	0.2%	1.3%	0.74%	0.57%	0.4%	0.34%	1.5%
Exact mass	5.9945	7.00099	7.99691	13.9969	14.0025	14.9984	15.9944	19.9806	21.9944

[a] Based on Earth isotopes abundances.

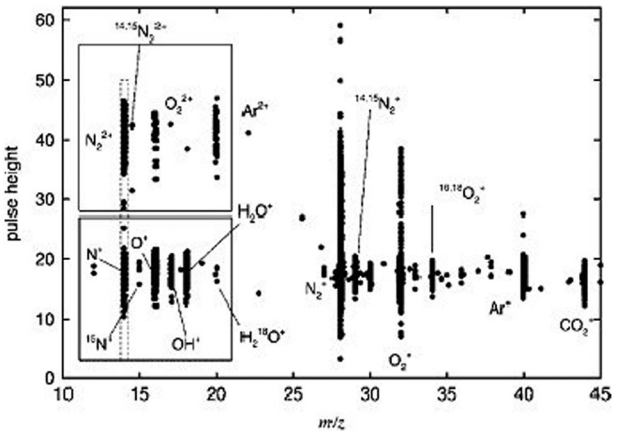

Fig. 10 Graph showing the ability to differentiate monocations and dications with identical m/q, when using a detector sensitive to ion energy. Reproduced from ref. 188 with permission from Wiley. Copyright 2008 Wiley.

an environment where it could detect such ions. Even though this would be the case, the overlap between N_2^{++} and N^+ is still indistinguishable. In order to separate these ions, one has to rely on specific detectors, able to distinguish the impulsion of ions, which is doubled when an ion is doubly-charged[188] (see Fig. 10 hereafter).

The doubly-charged ions which can be detected easily by mass spectrometry with medium resolution are atomic ions, as there is no m/q overlap with any other ion present in the atmospheres. Indeed, this technique allowed the detection of O^{++} ions at Venus, the Earth and Io, and of S^{++} at Io (see Section 2). Fig. 11 shows a measurement of O^{++} ions in the Earth's upper atmosphere, performed in 1974 at altitudes near 330 and 205 km, using the mass spectrometer MIMS on board Atmosphere Explorer C[11].

For molecular dications, the best candidate for detection with moderate-resolution instruments is the CO_2^{++} ion, though it has the same m/q as ^{22}Ne, a minor isotope (10%) of neon, a very minor constituent of atmospheres. Another possible route for detection by mass spectrometry is to make profit of the natural isotopes, which will produce small peaks seen at 0.5 u above the dication, and therefore present no overlap with singly charged ions. However this method requires improved sensitivity, as isotopic abundances barely reach 1.5% of mono-isotopical peaks (see Table 11).

4.2 Spectroscopy and remote sensing

The study of UV-Visible and IR light emissions observed in upper atmospheres of planets, also called airglow, is a very powerful way to infer information on atmospheric properties. This is also the case for the emissions arising from excited doubly-charged ions. Emission of atomic doubly-charged ions has been extensively used for temperature and density diagnostics in astrophysical sources (see for example the review of Keenan[189]) but only few observations have been made in planetary atmospheres (see Section 2). What we think are the most relevant emission multiplet lines in the 70–500 nm range for eventual detection of C^{++}, N^{++} and O^{++} ions in planetary atmospheres are tabulated in Table 12. Unfortunately, amongst the molecular ions that are discussed in the present review, only NO^{++} and N_2^{++} ions have known fluorescence transitions, which are summarised in Table 12.

O^{++} is by far the most abundant doubly-charged species in the Earth's ionosphere and is therefore the most likely to be detected optically. Several VUV emission lines of O^{++} have indeed been observed in aurorae or diurnal high-resolution emission spectra at 50.8, 52.6 and 70.3 nm.[12,13] The emissions at 495.8911 nm and 500.6843 nm have just recently been identified in VLT UVES spectra acquired in 2003.[36] The emissions near 166–167 nm may be identified in a spectrum acquired with the HUT telescope (see Fig. 12). However, more work is needed to confirm this challenging detection. It should be noted that while emission from excited O^{++} does indicate qualitatively that ground state O^{++} is present, the signal is actually giving information about the concentration of the excited state, and it is a relatively complex process to retrieve even relative concentrations of the ground state ion.

Due to the fast dissociation or predissociation of molecular dication excited states, fluorescence towards the ground state is expected to be a very rare phenomenon, but it was however observed in laboratory for N_2^{++} (see ref. 161, 162, 190 and 191). The bands were measured to be at 158.975 and 159.156 nm and correspond to the $D\ ^1\Sigma_u^+$–$X\ ^1\Sigma_g^+$ (0,0) and (0,1) transitions. The intensities of these emissions have been simulated for the Earth and Titan atmospheres and are predicted to be 0.6 and 0.2 Rayleigh (R), respectively, under solar minimum conditions.[25,28] They have not been detected so far. A search has been done with the Cassini UVIS data, shown in Fig. 13, which led to unsuccessful results, although an unidentified feature is present at around 159.7 nm, but it has not been clearly assigned to this transition.[193] New measurements by the same instrument in a Titan atmosphere exhibit a different aspect and were interpreted in terms of the Vegard Kaplan system.[194]

The emission band of NO^{++} at 256.3 nm has also been analyzed in laboratory, by Cossart *et al.*[168,169] It corresponds to the $B^2\Sigma^+$–$X^2\Sigma^+$ (0,0) transition. Fluorescent signal from the $A^2\Pi$–$X^2\Sigma^+$ transition is also reported by Besnard *et al.*,[159,167] but the photon energy is poorly constrained

 This journal is © the Owner Societies 2011

View Article Online

Published on 19 September 2011. Downloaded by BELGIAN INSTITUTE FOR SPACE AERONOMY on 11/02/2016 11:00:19.

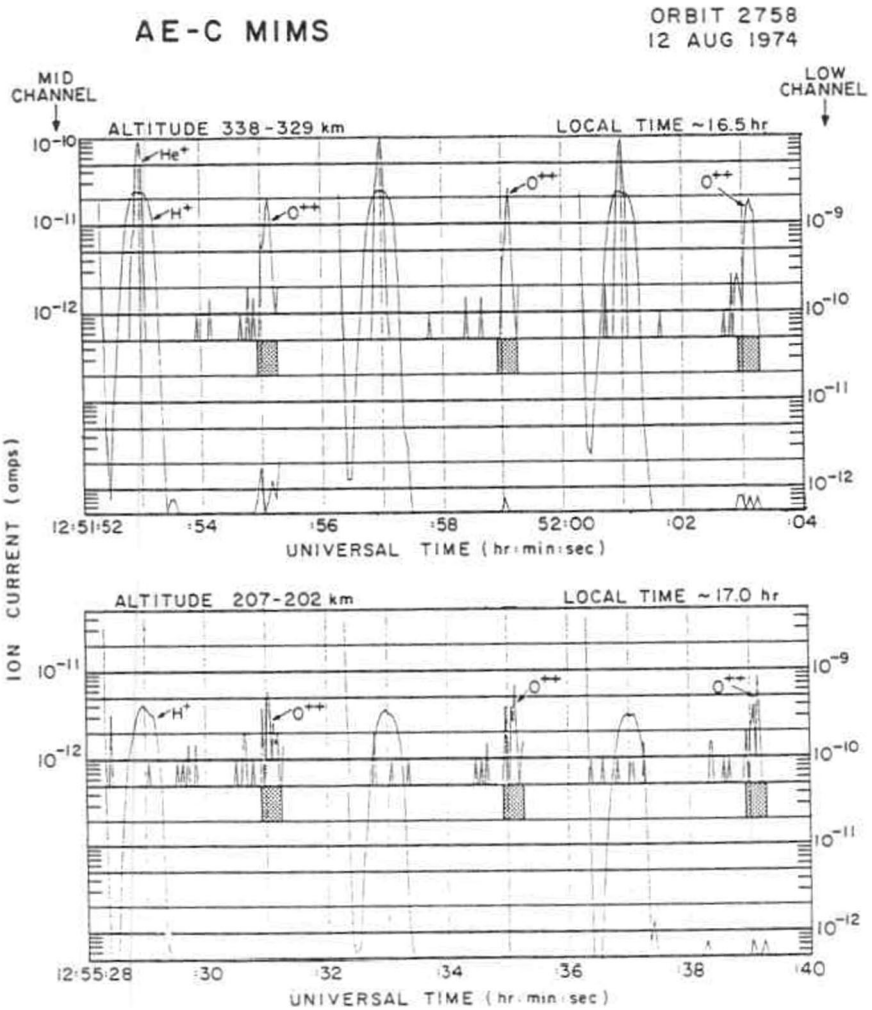

Fig. 11 Example of mass spectra recorded by the ion mass spectrometer MIMS instrument aboard the Atmospheric Explorer-C satellite (from Breig *et al.*,[11] copyright 1982 American Geophysical Union, reproduced by permission of American Geophysical Union). The instrument[5] is a magnetic ion-mass spectrometer designed to measure *in situ* the abundances of the ambient ion species in the mass range from 1 to 90 atomic mass units. Ion currents from the mid and low channels are referenced on the vertical axes. There is a clear signal for the O^{++} ion, which enabled the retrieval of reliable density profiles.

between 650 and 900 nm and Cox *et al.*[166] expect many lines to be populated due to the very different geometry between the two states. It is unlikely that these emissions may be detected in any atmosphere, due to the very low amount of NO.

Cossart and Robbe[144] have identified possible radiative transitions of CO^{++}. They correspond to the $^3\Sigma^+$–$X^3\Pi$ (0,0), (0,1) and (0,2) bands. The lists of wavelengths are reported in Table 12. It is unlikely that this emission may be detected in any atmosphere, due to the very low amount of CO. Let us note that this tentative identification was never confirmed, and that this prediction was even questioned recently by Mrugala.[135]

For O_2^{++}, no emission has been identified so far. Avakyan[30] reports the possible identification of auroral emissions around 243 nm which he assigns to the $A^3\Sigma^+$–$B^3\Pi_g$ transition. Three emission wavelengths have been tabulated by Avakyan *et al.*[31] based on previous calculated energies of O_2^{++} states[176,177] and reported in Table 12. Let us note that these values are given for completeness only, since no fluorescence of O_2^{++} has experimentally been confirmed yet, nor predicted by theoretical considerations, and the assignments tabulated by Avakyan had been assigned to emission lines from O^+ and O by Mahalingam and Hanson.[178] The fluorescence of O_2^{++} is certainly an area where progress is needed.

4.3 Ionospheric density budget

The neutrality of a planetary ionosphere requests that the density of negative charges is equal to the density of positive charges. A challenging way for detecting very small densities of doubly-charged ions would consist in measuring the density of all electrons and of all ions (neglecting information on the charge, q). An excess of negative charges could then be attributable to the contribution of doubly-charged ions. This is very challenging as it implies to measure the plasma density with an extreme accuracy, since the doubly-charged ions represent less than 1% of the total density. As an example, the ratio O^{++} over electron density is around 0.1% in the Earth atmosphere at 600 km and is similar in the Venus atmosphere at 250 km. The required accuracy is of the order of a few particles per cm^3.

View Article Online

Published on 19 September 2011. Downloaded by BELGIAN INSTITUTE FOR SPACE AERONOMY on 11/02/2016 11:00:19.

Table 12 List of emissions of doubly-charged ions of relevant importance in the upper atmosphere of planets

Species	Wavelength/nm	Transition	Ref.
C^{++}	72.7262	$^3P–^1S$	49
	72.7514		
	97.703	$^1P–^1S$	
	190.6683	$^3P–^1S$	
	190.8734		
	199.9953	$^1P–^3P$	
	200.0901		
	200.3161		
N^{++}	76.3334	$^2S–^2P$	49
	76.4351		
	98.9790	$^2D–^2P$	
	99.1514		
	99.1579		
	174.6823	$^4P–^2P$	
	174.8646		
	174.9674		
	175.2160		
	175.3995		
	464.064	$^2D–^2P$	
O^{++}	70.2337	$^3P–^3P$	49
	70.2838		
	70.2896		
	70.2900		
	70.3850		
	70.3854		
	83.2929	$^3D–^3P$	
	83.3715		
	83.3749		
	83.5059		
	83.5092		
	83.5289	$^5S–^3P$	
	166.0809		
	166.6150	$^1S–^3P$	
	232.0951		
	233.1398	$^1S–^1D$	
	436.3209	$^1D–^3P$	
	493.1227		
	495.8911		
	500.6843		
CO^{++}	492.36[a]	$^3\Sigma^+–X^3\Pi$ (0,0)[a]	Tentatively reported
	490.95[a]	$^3\Sigma^+–X^3\Pi$ (0,0)[a]	by Cossart and
	530.24[a]	$^3\Sigma^+–X^3\Pi$ (0,1)[a]	Robbe[144] but this
	528.58[a]	$^3\Sigma^+–X^3\Pi$ (0,1)[a]	work was
	569.59[a]	$^3\Sigma^+–X^3\Pi$ (0,2)[a]	questioned by
	567.68[a]	$^3\Sigma^+–X^3\Pi$ (0,2)[a]	Mrugala *et al.*[135]
N_2^{++}	158.975	$D^1\Sigma_u^+–X\ ^1\Sigma_g^+$ (0,0)	161, 162, 190
	159.156	$D^1\Sigma_u^+–X\ ^1\Sigma_g^+$ (1,1)	and 191
	163.5	$D^1\Sigma_u^+–X\ ^1\Sigma_g^+$ (2,3)	
NO^{++}	256.30	$B^2\Sigma^+–X\ ^2\Sigma^+$ (0,0)	168 and 169
O_2^{++}	417[a]	$A^3\Sigma^+–B^3\Pi g$[a]	31 and 178
	443[a]		
	470[a]		

[a] Controversial (see the text).

5. Applications of dications in atmospheres

As shown in the potential energy curves of the molecular dications considered in this study (Section 3.1), many molecular dications exhibit a potential energy well in their ground electronic states, due to a barrier which prevents their exothermic dissociation into two singly charged fragments to occur spontaneously. This particular behaviour, *i.e.* stability and propensity for high energy release lead to astonishing hypotheses, such as the use of He_2^{++} as a base product for high energy fuel.[195] The difficulty to stabilize macroscopic quantities of molecular dications in condensed media however precluded any sound application of the concept. The gas-phase chemistry of the dications is hence exceptional in its ability to release energy and therefore induces, when the right reactants are considered, exotic behaviour, in some respect similar to the one observed in the very innovative condensed phase carbo-dication chemistry.[196]

5.1 Exotic chemistry

Gas-phase reactions of doubly-charged ions have been studied in the laboratory mainly for atomic ions. Doubly-charged molecular ions became accessible to experimentalists thanks to coincidence methods, as well as instruments with improved sensitivity.

The main reactive channels are due to charge transfer, either dissociative or non-dissociative. Only single charge transfer is observed, the double charge transfer being negligible. This is not surprising, as one expects charge transfer to be very efficient at large internuclear distances. Dissociation induced by collision is a limited process. This was not expected, as molecular doubly-charged ions are only metastable towards their exothermic dissociation into singly charged fragments. It was therefore expected that collision would induce their dissociation. However, this is not the case for collision energies up to 10 eV. This indicates that the energy transfer process is inefficient, compared to the charge transfer process.

Bond forming reactions have been searched for and reported, for example in the reactions of CO_2^{++} with CO_2 giving some O_2^+ product ions,[184] or N_2^{++} with O_2 producing NO^+,[164] or N_2^{++} with CH_4 and C_2H_4 producing HCN^+ and $HCNH^+$. These chemical reactions require a long-lived intermediate complex for atoms to rearrange. They are described in the frame of the Landau–Zener "reaction window" model and represent only minor channels for doubly charged ion reactions.

Since the 1990s, some works have shown that exotic or unexpected chemistry could be observed when dealing with doubly-charged ions. There are three recent reviews on the subject (see ref. 197–199). Recently, a few papers have reported experimental studies on reactions of doubly-charged molecular ions, in particular for CO_2^{++} (see ref. 46, 127 and 185), N_2^{++} (see ref. 164) and O_2^{++} (see ref. 127), expected to be present in planetary atmospheres. The internal energy effect on such reactions has only been studied in the case of CO_2^{++} ion reactions.[184] The product branching ratio between products has been observed to vary with the CO_2^{++} internal energy. This is again surprising because of the very small variation of the total energy content when adding some internal energy in the parent ion. It has been interpreted as the possible result of the internuclear distance variation with increasing electronic or vibrational energy. However, in planetary atmospheres, very few excited states of molecular doubly charged ions have a lifetime which is long enough to allow their decay by reactions. So this effect can be neglected in most cases.

In 2008, the reactivity of molecular dications, generated by double ionisation of different aromatic or hetero-aromatic compounds, was shown to activate methane and undergo

 This journal is © the Owner Societies 2011

View Article Online

Published on 19 September 2011. Downloaded by BELGIAN INSTITUTE FOR SPACE AERONOMY on 11/02/2016 11:00:19.

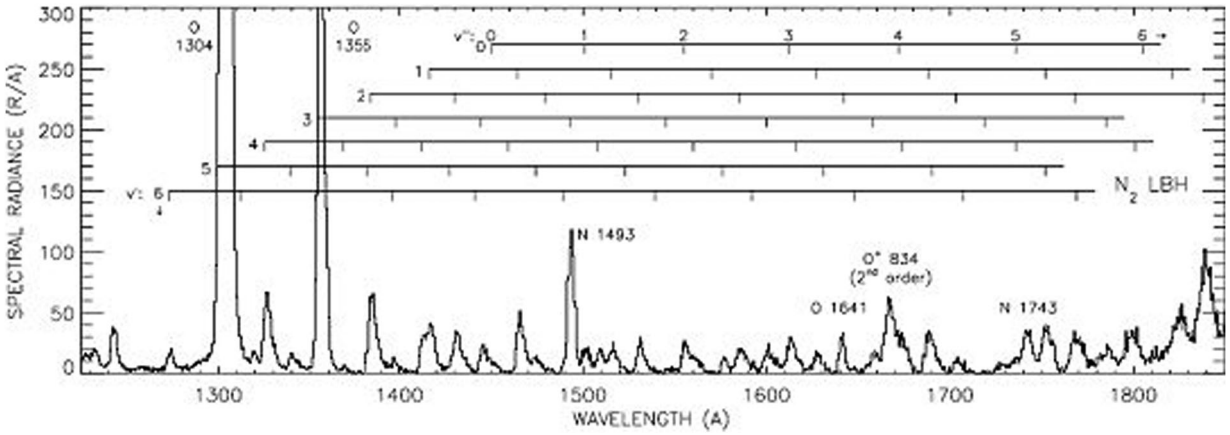

Fig. 12 From Bishop and Feldman,[192] (copyright 2003 American Geophysical Union, reproduced by permission of American Geophysical Union), showing a spectrum of the Earth atmosphere in the EUV–FUV range. The emissions near 166–167 nm of O^{++} may be potentially identified.

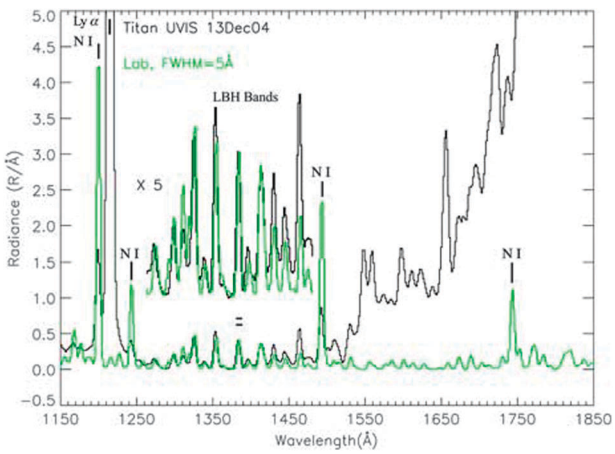

Fig. 13 Titan spectrum from Ajello *et al.*[193] (copyright 2007 American Geophysical Union, reproduced by permission of American Geophysical Union), covering the range 115–185 nm. A feature around 159.7 nm is still unidentified.

carbon–carbon coupling reactions, therefore leading to molecular growth. The potential relevance of these results was discussed in the context of the growth of hydrocarbon species and their nitrogen-containing homologues, in particular in the ionospheric conditions observed in Saturn's moon Titan.[45–48,199,200]

In conclusion, the experimental results on the few reactions of molecular doubly-charged ions which have been experimentally studied so far show that it is very difficult at the present stage to predict the ion products of such reactions. More laboratory work is therefore essential for all reactions which can occur in planetary upper atmospheres.

5.2 Atmospheric escape

One consequence of the exotic behaviour of doubly-charged ions in planetary atmospheres is the possibility of creation of dissociative products with a kinetic energy of several eV. This energy is large enough in the case of Mars and Titan to allow these fragments to reach sufficient velocity to escape into space (see Table 13). Therefore this process can in principle contribute to the continuous erosion of these atmospheres. Let us consider the case of CO_2^{++}. Two processes can lead to the release of fragments with high kinetic energy (see Section 3.1 for further details). The dissociative double photoionisation of CO_2 releases CO^+ and O^+, with a total kinetic energy release (KER) between 3 and 6 eV, depending on the photon energy.[183] Considering the maximum of this KER distribution, it gives a most probable value of 4 and 2 eV kinetic energy for O^+ and CO^+, respectively. The dissociative recombination of CO_2^{++} with electrons follows different energetically allowed channels with a total exothermicity up to 18.1 eV.[132] As a third process, the charge exchange does not liberate fragments with a significant kinetic energy.

The modelling of escape fluxes of these fragments can be carried out as follows (*e.g.* ref. 201–203): the velocity distribution of the fragments is computed, with the knowledge of the densities of the main neutral and ionised atmospheric components, the solar flux (which depends on the solar activity), the relevant photoionisation cross-sections and dissociative recombination rate coefficients (which depend on the electron temperature), and the branching ratio for the different channels. The result indicates which fraction of the fragments possesses a velocity higher than the escape velocity. The global escape rate is computed by integrating the rate above the exobase, the atmospheric boundary above which the species may escape.

The computation of escape due to double ionisation (dissociative or *via* recombination) is complex as outlined in the previous paragraph and is beyond the scope of this review paper, therefore no quantitative results are given here. It is important to mention that in the case of Mars (and most likely Titan), because of the low escape velocity, photochemical

Table 13 Typical escape energy (eV) for the C^+, N^+ and O^+ ions in the atmosphere of Venus, Earth, Mars and Titan, at the exobase

Ion/planet	Venus	Earth	Mars	Titan
C^+	6.4	7.4	1.5	0.28
N^+	7.5	8.6	1.8	0.32
O^+	8.6	9.8	2.0	0.37

View Article Online

Published on 19 September 2011. Downloaded by BELGIAN INSTITUTE FOR SPACE AERONOMY on 11/02/2016 11:00:19.

processes involving doubly-charged ions must lead to atmospheric escape, whose fluxes are expected to be low, but non-negligible, and strongly dependent on the solar activity.

5.3 Diagnostic of the neutral atmosphere

Potential presence of doubly-charged molecular ions is hardly considered in mass spectrometry. It could be used to help in the detection of abundant molecular species, which, when probed directly, present the risk of saturation of the detector. For example, the quantification of HCN in Titan's upper atmosphere[204] is very difficult[205] because the molecular monocation resulting from 70 eV electron ionisation of HCN is at $m/q = 27$, very close to the intense peak at $m/q = 28$ resulting from molecular nitrogen ionisation. As HCN exhibits a stable (microsecond lifetime) dication,[206] which should be observed at $m/q = 13.5$, a slight improvement of resolution and detuning of the standard acquisition procedure in order to probe specifically ions at half mass unit could therefore be an unexpected help in quantification of the HCN molecule in the Titan atmosphere.

6. Numerical modelling of the ionospheres, including doubly-charged ions

Numerical modelling is a powerful tool for studying planetary ionospheres, since it allows us to analyze and constrain the physical and chemical mechanisms at work, by comparing with data. Kinetic and fluid formalisms are used to describe the different plasma populations: ions, electrons, thermal and suprathermal components. Depending on the complexity of the models, the following macroscopic parameters can be computed: plasma densities, velocities, temperatures. The magnetic field can be added and self-computed if required. The models can be run in one to three dimensions, day and/or night conditions, for various seasons and solar activities.

Simulations of stable doubly-charged ions densities have been performed for Venus, Mars, Earth and Titan, and a summary plot is displayed below: the results of simulations shown in Fig. 14, for simplicity, assumed that the doubly-charged ions are in photochemical equilibrium. In other words, the density is computed by assuming that the chemical losses equal the photo-chemical productions. This assumption is valid over a certain range of altitudes (in the case of Mars, around the maximum electron density peak at about 130–140 km altitude). The ion density is thus computed with the known production and loss processes. In those models, double photoionisation or electron ionisation cross sections have been included only for the production of stable molecular doubly-charged ions in ionospheric conditions (lifetimes longer than a second). Dissociative double ionisation cross sections have not been included, even though they have much higher values, because

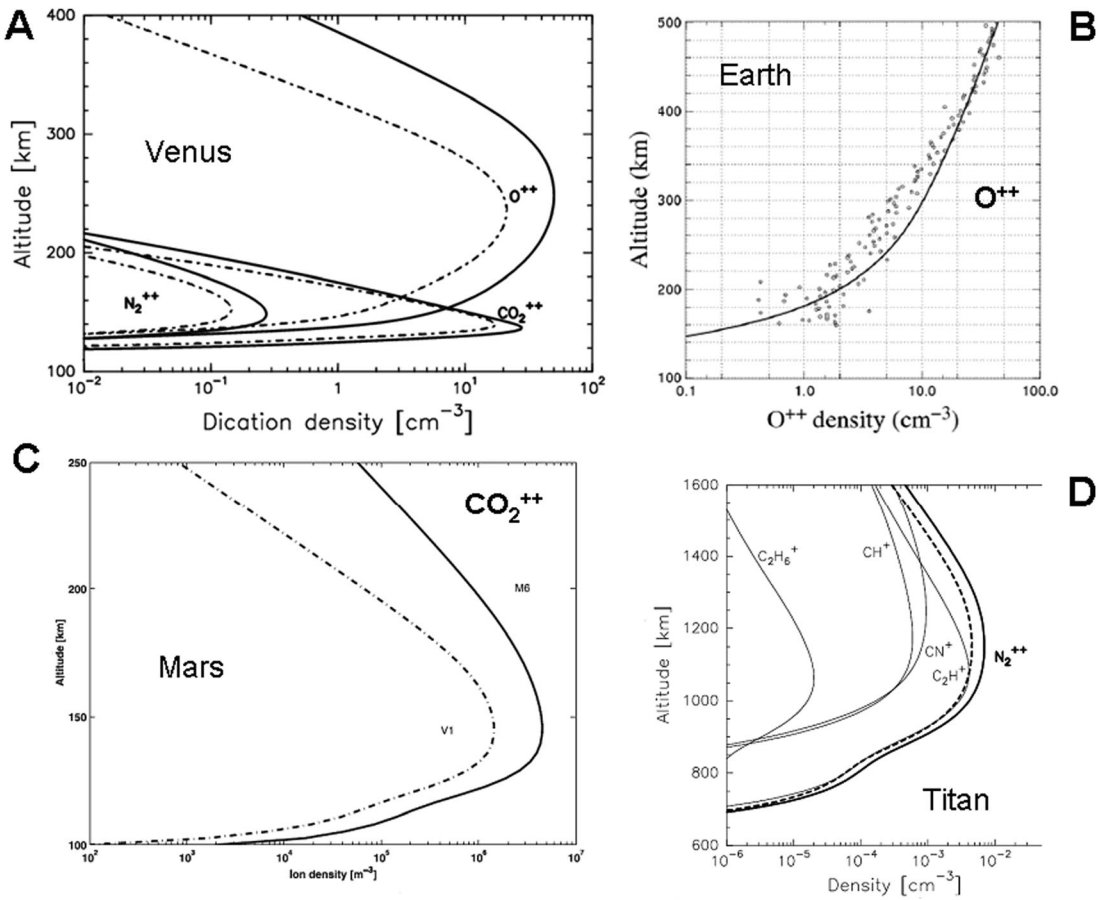

Fig. 14 Examples of results from numerical simulations of the densities of doubly-charged ions in the ionospheres of Venus (panel A, reproduced from ref. 29 by permission of European Southern Observatory, copyright 2007 ESO), Earth (panel B, reproduced from ref. 25 by permission of European Geophysical Union, copyright 2005 EGU), Mars (panel C, reproduced from ref. 26 and 27 by permission of American Geophysical Union, copyright 2003 AGU) and Titan (panel D, reproduced from ref. 28 by permission of American Geophysical Union, copyright 2005 AGU).

 This journal is © the Owner Societies 2011

View Article Online

Published on 19 September 2011. Downloaded by BELGIAN INSTITUTE FOR SPACE AERONOMY on 11/02/2016 11:00:19.

the study was focused on the calculation of molecular dication densities. Loss processes of molecular dications include ion molecule reactions and recombination with electrons. In Fig. 14, one can see that the densities vary a lot depending on the species and on the planet, because of the different atmospheric compositions and heliocentric distances. To give an example, the N_2^{++} ion density peak is 10^{-1} cm^{-3} at 140 km at Venus, while it reaches 10^{-2} cm^{-3} at 1150 km at Titan. When measurements are available, as it is the case for Venus and the Earth for O^{++}, it is very interesting to test whether the physical and chemical parameters measured in laboratory can be used as valid inputs in the model.

For Mars, Fig. 15 displays the densities of five ions, including non-dissociative CO_2^{++}. The doubly-charged ion density reaches its maximum at about 140 km. The peak density is well below the density of the major ions; nevertheless it could be detected with a dedicated mass spectrometer.

For completeness, one should mention the modelling efforts performed at Venus by Fox and Victor,[37] which allowed us to constrain the rate coefficient for the reaction between O and O^{++}. For the Earth, several publications deal with this topic: Breig *et al.*[6,11] developed a model of O^{++} and explored in detail its photochemistry. Truhlik[16] proposed an explanation for the strong density variations of O^{++} in the outer ionosphere in period of geomagnetic storm, by invoking the key influence of H^+ ion fluxes.

7. Needs, next steps, challenges

7.1 Laboratory experiments

From Section 3.1 of this review, it is possible to derive the experimental information that is missing to describe more accurately the dications in planetary atmospheres.

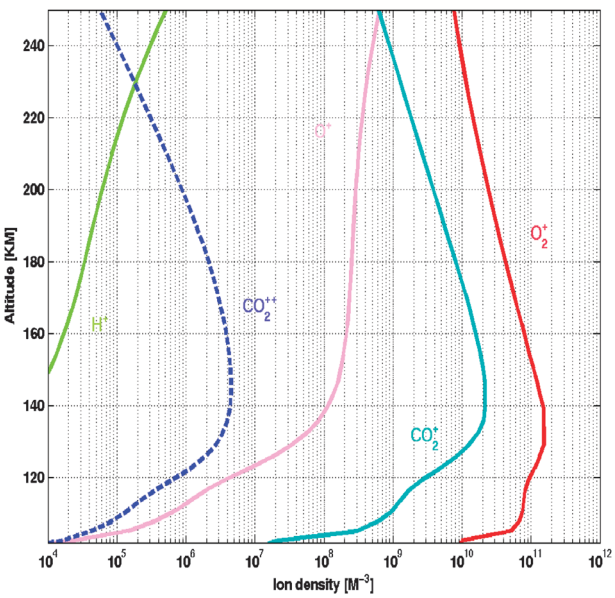

Fig. 15 Model of the ionosphere of Mars developed by the authors. The major ions (O_2^+, CO_2^+ and O^+) are shown. The doubly-charged ion CO_2^{++} densities are plotted for comparison. Another minor ion, H^+, is also plotted.

Among production processes, there is the need to measure the double photoionisation cross section of O_2 and the electron double ionisation cross section of NO. The singly charged ion ionisation cross section by photon is missing for O_2^+, NO^+ and CO_2^+, and similar data for electron ionisation are missing for NO^+.

Among loss processes, the dissociative recombination is missing for O_2^{++} and NO^{++}. The reactivity is often qualitatively described, but there is a need for more quantitative (cross section or better rate constant) measurements, in the energy range corresponding to 0–1 eV. Particularly useful would be a study of the reactivity of CO^{++} with O_2 and of N_2^{++} with CH_4.

Natural lifetime is an important issue; it requests very specific experimental tools to measure it, such as ion rings. It is missing for NO^{++}, and O_2^{++}.

It is also clear that the potential remote detection of dications through their emission is a promising route, and requests for well established spectroscopic information (line positions and cross sections). The CO^{++} and O_2^{++} fluorescence is not well established, and let us mention that high resolution rotational spectra of CO^{++}, NO^{++}, and CO_2^{++} can be expected, and would be very valuable in the near future to take advantage of the high resolution surveys now collected, or soon to be, by space observatories such as Herschel or Alma.

Hopefully, the requested data will be measured in near future, and will be compiled in the Kinetic Database of Astrophysics (KIDA http://kida.obs.u-bordeaux1.fr). KIDA is a database of kinetic data of interest for astrochemical (interstellar medium and planetary atmospheres) studies. In addition to the available referenced data, KIDA provides recommendations over a number of important reactions. It has been implemented to incorporate information on doubly-charged species.

7.2 Flight hardware design

We can wish that any future planetary missions will embark space instrumentation able to detect doubly-charged ions. The detectability of these species is discussed in Section 4. We strongly recommend studying the design of the following types of instruments:

- Ion mass spectrometers with the following performances: (i) either improved resolution mass spectrometers with excellent detection dynamics (better than 4 orders of magnitude), giving access to the non-integer mass to charge peaks resulting unequivocally from doubly-charged ions (for the considered ions, this would imply a separation of 0.5 u up to $m/q = 23$ in order to extract signal from $^{13}CO^{++}$, $^{14}N^{15}N^{++}$, $^{15}NO^{++}$ and $^{13}CO_2^{++}$), (ii) mass spectrometers with specific detectors optimised for differentiation of charge, based on the impact energy of ionic species.

- Spectrometers or spectrograph covering the relevant range in Table 12 in Section 4.2, *i.e.* from 70 to 900 nm. Obviously the range must be adapted planet by planet. The sensitivity would be typically better than 100 Rayleigh per nm, while the spectral resolution must be better than 0.3 nm.

As mentioned in Section 4, one way of detecting the doubly-charged ion is to measure accurately the ionospheric

View Article Online

Published on 19 September 2011. Downloaded by BELGIAN INSTITUTE FOR SPACE AERONOMY on 11/02/2016 11:00:19.

density budget. To this end, one would need a dedicated ion and electron spectrometer able to measure plasma density with accuracy of the order of a few particles per cm^{-3}.

7.3 Suggested data analysis in the near future

As written in the previous section, a new generation of missions and flight hardware is needed to make huge progress in the detection of doubly-charged ions in planetary atmospheres, requiring either improved resolution, or specific detection. However, an enormous data set exists for all planets, including our Earth. Data archive 'mining' offers the potential for discoveries, and we suggest here a few ideas, for Venus, Earth, Mars and Titan.

At Venus, Venus Express ASPERA4 data (*e.g.* ref. 207) offer the potential to confirm the detection of O^{++} ions and to further describe the variability of its density, as a function of solar activity. The mass resolution of this instrument is most likely not sufficient to measure the ion without ambiguity. However, by considering predicted doubly-charged ion[37] in the data processing, some useful data could be retrieved. CO_2^{++} density is expected to peak at 140 km on the dayside, and could be studied further with a careful analysis of the NASA Pioneer Venus Orbiter dataset. For the Earth, what needs to be done in priority is clearly to detect the O_2^{++} and N_2^{++} doubly-charged ions, most likely with a new generation of mass spectrometers able to distinguish the doubly-charged molecular ion from the singly-charged atomic ion. An interesting possibility would be to attempt to detect the emissions in the UV and visible ranges, with spectrographic data. Information on the still undetected emissions of O^{++} might be hidden in some data sets. At Mars, the most promising discovery would be the confirmation of detection of O^{++} ions in the data from the Mars Express ASPERA3 data sets.[38] At Titan, the Cassini INMS mass spectrometer[204] and UVIS UV spectrometer[193,208] datasets constitute a mine to explore. As a general remark, the data analysis could focus on periods of high solar activity or exceptional solar events such as eruption, coronal mass ejections, ENA, intense proton precipitation, *etc.*, during which strong enhancement of the doubly-charged ion density can be expected.

Acknowledgements

Since 10 years, our studies of doubly-charged ions in planetary ionospheres have received constant and precious support from the French Programme National de Planétologie, which is here acknowledged. The work of Guillaume Gronoff was supported by an appointment of the NASA Postdoctoral Program at NASA Langley Research Center, administered by Oak Ridge Associated Univ. through a contract with NASA, and funded by the NASA Science Mission Directorate.

References

1 H. B. Niemann, S. K. Atreya, J. E. Demick, D. Gautier, J. A. Haberman, D. N. Harpold, W. T. Kasprzak, J. I. Lunine, T. C. Owen and F. Raulin, *J. Geophys. Res.*, 2010, **115**, 12006.
2 R. J. Mawhorter, A. Chutjian, T. E. Cravens, N. Djuric, S. Hossain, C. M. Lisse, J. A. Macaskill, S. J. Smith, J. Simcic and I. D. Williams, *Phys. Rev. A: At., Mol., Opt. Phys.*, 2007, **75**, 32704.
3 J. H. Hoffman, C. Y. Johnson, J. C. Holmes and J. M. Young, *J. Geophys. Res.*, 1969, **74**, 6281–6290.
4 H. A. Taylor, Jr., *J. Geophys. Res.*, 1973, **78**, 315–319.
5 J. H. Hoffman, W. H. Dodson, C. R. Lippincott and H. D. Hammack, *J. Geophys. Res.*, 1974, **79**, 4246–4251.
6 E. L. Breig, W. B. Hanson, J. H. Hoffman, M. R. Torr, D. G. Torr, J. C. G. Walker and A. O. Nier, *J. Geophys. Res.*, 1977, **82**, 1008–1012.
7 D. T. Young, J. Geiss, H. Balsiger, P. Eberhardt, A. Ghielmetti and H. Rosenbauer, *Geophys. Res. Lett.*, 1977, **4**, 561–564.
8 S. V. Avakyan, *Cosmic Res.*, 1980, **17**, 786–789.
9 H. Balsiger, P. Eberhardt, J. Geiss and D. T. Young, *J. Geophys. Res.*, 1980, **85**, 1645–1662.
10 H. Balsiger, P. Eberhardt, J. Geiss and D. T. Young, *J. Geophys. Res.*, 1980, **85**, 6080–6080.
11 E. L. Breig, M. R. Torr and D. C. Kayser, *J. Geophys. Res.*, 1982, **87**, 7653–7665.
12 F. Paresce, S. Chakrabarti, R. Kimble and S. Bowyer, *J. Geophys. Res., [Space Physics]*, 1983, **88**, 247–252.
13 E. P. Gentieu, P. D. Feldman, R. W. Eastes and A. B. Christensen, *J. Geophys. Res., [Space Physics]*, 1984, **89**, 1053–1058.
14 J. Boskova, V. Truhlik, J. Smilauer and P. Triska, *J. Atmos. Terr. Phys.*, 1996, **58**, 867–874.
15 J. Smilauer, V. Truhlik, J. Boskova, P. Triska and J. Schultchishin, *Adv. Space Res.*, 1996, **17**, 135–140.
16 V. Truhlik, *Adv. Space Res.*, 1997, **20**, 419–423.
17 H. A. Taylor, H. C. Brinton, T. C. G. Wagner, B. H. Blackwell and G. R. Cordier, *IEEE Trans. Geosci. Remote Sens.*, 1980, **18**, 44–49.
18 S. Ghosh, K. K. Mahajan, J. M. Grebowsky and N. Nath, *J. Geophys. Res.*, 1995, **100**, 23983–23992.
19 L. A. Frank, W. R. Paterson, K. L. Ackerson, V. M. Vasyliunas, F. V. Coroniti and S. J. Bolton, *Science*, 1996, **274**, 394–395.
20 L. A. Frank and W. R. Paterson, *J. Geophys. Res.*, 2001, **106**, 6131–6149.
21 P. D. Feldman, D. F. Strobel, H. W. Moos and H. A. Weaver, *Astrophys. J.*, 2004, **601**, 583–591.
22 S. S. Prasad and D. R. Furman, *J. Geophys. Res.*, 1975, **80**, 1360–1362.
23 S. V. Avakyan, *Cosmic Res.*, 1978, **16**, 115–119.
24 S. V. Avakyan, *Geomagn. Aeron. (Engl. Transl.)*, 1979, **18**, 652–655.
25 C. Simon, J. Lilensten, O. Dutuit, R. Thissen, O. Witasse, C. Alcaraz and H. Soldi-Lose, *Ann. Geophys.*, 2005, **23**, 781–797.
26 O. Witasse, O. Dutuit, J. Lilensten, R. Thissen, J. Zabka, C. Alcaraz, P. L. Blelly, S. W. Bougher, S. Engel, L. H. Andersen and K. Seiersen, *Geophys. Res. Lett.*, 2002, **29**, 104.
27 O. Witasse, O. Dutuit, J. Lilensten, R. Thissen, J. Zabka, C. Alcaraz, P. L. Blelly, S. W. Bougher, S. Engel, L. H. Andersen and K. Seiersen, *Geophys. Res. Lett.*, 2003, **30**, 12.
28 J. Lilensten, O. Witasse, C. Simon, H. Soldi-Lose, O. Dutuit, R. Thissen and C. Alcaraz, *Geophys. Res. Lett.*, 2005, **32**, 03203.
29 G. Gronoff, J. Lilensten, C. Simon, O. Witasse, R. Thissen, O. Dutuit and C. Alcaraz, *Astron. Astrophys.*, 2007, **465**, 641–645.
30 S. V. Avakyan, *Geomagn. Aeron. (Engl. Transl.)*, 1978, **18**, 444–446.
31 S. V. Avakyan, *J. Opt. Technol.*, 1998, **65**, 870–875.
32 *Collision processes and excitation of UV emission from planetary atmospheric gases: a handbook of cross sections*, ed. S. V. Avakyan, R. N. Il'in, V. M. Lavrov and G. N. Ogurtsov, Gordon and Breach Science Publishers, London, 1998.
33 G. A. Victor and E. R. Constantinides, *Geophys. Res. Lett.*, 1979, **6**, 519–522.
34 S. V. Avakyan and M. G. Deminov, *Kosm. Issled.*, 1983, **21**, 806–810.
35 J. Geiss, H. Balsiger, P. Eberhardt, H. P. Walker, L. Weber, D. T. Young and H. Rosenbauer, *Space Sci. Rev.*, 1978, **22**, 537–566.
36 O. Witasse, T. Slanger and R. Thissen, *Ann. Geophys.*, 2011, accepted.

 This journal is © the Owner Societies 2011

View Article Online

Published on 19 September 2011. Downloaded by BELGIAN INSTITUTE FOR SPACE AERONOMY on 11/02/2016 11:00:19.

37 J. L. Fox and G. A. Victor, *J. Geophys. Res.*, 1981, **86**, 2438–2442.
38 E. Dubinin, R. Modolo, M. Fraenz, J. Woch, G. Chanteur, F. Duru, F. Akalin, D. Gurnett, R. Lundin, S. Barabash, J. D. Winningham, R. Frahm, J. J. Plaut and G. Picardi, *J. Geophys. Res.*, 2008, **113**, 10217.
39 A. L. Broadfoot, M. J. Belton, P. Z. Takacs, B. R. Sandel, D. E. Shemansky, J. B. Holberg, J. M. Ajello, H. W. Moos, S. K. Atreya, T. M. Donahue, J. L. Bertaux, J. E. Blamont, D. F. Strobel, J. C. McConnell, R. Goody, A. Dalgarno and M. B. McElroy, *Science*, 1979, **204**, 979–982.
40 B. R. Sandel and A. L. Broadfoot, *J. Geophys. Res.*, 1982, **87**, 2231–2240.
41 B. R. Sandel and A. L. Broadfoot, *J. Geophys. Res.*, 1982, **87**, 212–218.
42 A. J. Steffl, P. A. Delamere and F. Bagenal, *Icarus*, 2006, **180**, 124–140.
43 F. L. Roesler, F. Scherb and R. J. Oliversen, *Geophys. Res. Lett.*, 1984, **11**, 128–130.
44 J. L. Linsky, H. Yang, K. France, C. S. Froning, J. C. Green, J. T. Stocke and S. N. Osterman, *Astrophys. J.*, 2010, **717**, 1291–1299.
45 C. L. Ricketts, D. Schroder, C. Alcaraz and J. Roithova, *Chem.–Eur. J.*, 2008, **14**, 4779–4783.
46 C. L. Ricketts, D. Schröder, J. Roithova, H. Schwarz, R. Thissen, O. Dutuit, J. Zabka, Z. Herman and S. D. Price, *Phys. Chem. Chem. Phys.*, 2008, **10**, 5135.
47 E. L. Zins, C. Pepe and D. Schröder, *Faraday Discuss.*, 2010, **145**, 157–169.
48 E. L. Zins and D. Schröder, *J. Phys. Chem. A*, 2010, **114**, 5989–5996.
49 Y. Ralchenko, A. E. Kramida, J. Reader and N. A. Team, *NIST Atomic Spectra Database (version 4.0)*, National Institute of Standards and Technology, Gaithersburg, MD, available: http://physics.nist.gov/asd, 2010.
50 M. D. Ward, S. J. King and S. D. Price, *J. Chem. Phys.*, 2011, **134**, 4308.
51 D. Stahl, F. Maquin, T. Gaumann, H. Schwarz, P. A. Carrupt and P. Vogel, *J. Am. Chem. Soc.*, 1985, **107**, 5049–5053.
52 J. H. D. Eland, M. Hochlaf, G. C. King, P. S. Kreynin, R. J. LeRoy, I. R. McNab and J.-M. Robbe, *J. Phys. B: At., Mol. Opt. Phys.*, 2004, **37**, 3197–3214.
53 M. Ahmad, P. Lablanquie, F. Penent, J. G. Lambourne, R. I. Hall and J. H. D. Eland, *J. Phys. B: At., Mol. Opt. Phys.*, 2006, **39**, 3599–3616.
54 J. Eland, *Chem. Phys.*, 2003, **290**, 27–34.
55 R. I. Hall, G. Dawber, A. McConkey, M. A. MacDonald and G. C. King, *Phys. Rev. Lett.*, 1992, **68**, 2751–2754.
56 A. E. Slattery, T. A. Field, M. Ahmad, R. I. Hall, J. Lambourne, F. Penent, P. Lablanquie and J. H. D. Eland, *J. Chem. Phys.*, 2005, **122**, 4317.
57 R. D. Molloy, A. Danielsson, L. Karlsson and J. H. D. Eland, *Chem. Phys.*, 2007, **335**, 49–54.
58 S. L. Carter and H. P. Kelly, *J. Phys. B: At. Mol. Phys.*, 1976, **9**, 1887–1897.
59 J. A. R. Samson and G. C. Angel, *Phys. Rev. A: At., Mol., Opt. Phys.*, 1990, **42**, 1307.
60 J. A. Fennelly and D. G. Torr, *At. Data Nucl. Data Tables*, 1992, **51**, 321.
61 J. A. R. Samson, Z. X. He, R. Moberg, W. C. Stolte and J. N. Cutler, *Can. J. Phys.*, 1996, **74**, 722.
62 P. Franceschi, D. Ascenzi, P. Tosi, R. Thissen, J. Zabka, J. Roithova, C. L. Ricketts, M. de Simone and M. Coreno, *J. Chem. Phys.*, 2007, **126**, 4310.
63 W. C. Stolte, Z. X. He, J. N. Cutler, Y. Lu and J. A. R. Samson, *At. Data Nucl. Data Tables*, 1998, **69**, 171.
64 G. C. Angel and J. A. R. Samson, *Phys. Rev. A: At., Mol., Opt. Phys.*, 1988, **38**, 5578–5585.
65 G. Dujardin, D. Winkoun and S. Leach, *Phys. Rev. A: At., Mol., Opt. Phys.*, 1985, **31**, 3027–3038.
66 T. Masuoka and E. Nakamura, *Phys. Rev. A: At., Mol., Opt. Phys.*, 1993, **48**, 4379–4389.
67 R. Wehlitz, *Adv. At., Mol., Opt. Phys.*, 2010, **58**, 1–76.
68 J. A. R. Samson, T. Masuoka and P. N. Pareek, *J. Chem. Phys.*, 1985, **83**, 5531–5535.
69 T. Masuoka, *Phys. Rev. A: At., Mol., Opt. Phys.*, 1993, **48**, 1955–1963.
70 M. Alagia, P. Candori, S. Falcinelli, M. Lavollée, F. Pirani, R. Richter, S. Stranges and F. Vecchiocattivi, *J. Phys. Chem. A*, 2009, **113**, 14755–14759.
71 T. Masuoka, *Phys. Rev. A: At., Mol., Opt. Phys.*, 1994, **50**, 3886–3894.
72 E. M. Bahati, J. J. Jureta, D. S. Belic, H. Cherkani-Hassani, M. O. Abdellahi and P. Defrance, *J. Phys. B: At., Mol. Opt. Phys.*, 2001, **34**, 2963–2973.
73 Y. Itikawa and A. Ichimura, *J. Phys. Chem. Ref. Data*, 1990, **19**, 637–651.
74 W. R. Thompson, M. B. Shah and H. B. Gilbody, *J. Phys. B: At., Mol. Opt. Phys.*, 1995, **28**, 1321–1330.
75 B. G. Lindsay, R. Rejoub and R. F. Stebbings, *J. Chem. Phys.*, 2001, **114**, 10225–10226.
76 C. Tian and C. R. Vidal, *Phys. Rev. A: At., Mol., Opt. Phys.*, 1999, **59**, 1955–1965.
77 J. Gavin, M. Ortiz and J. Campos, *Int. J. Mass Spectrom.*, 2002, **219**, 351–361.
78 C. Tian and C. R. Vidal, *J. Phys. B: At., Mol. Opt. Phys.*, 1998, **31**, 5369–5381.
79 H. C. Straub, P. Renault, B. G. Lindsay, K. A. Smith and R. F. Stebbings, *Phys. Rev. A: At., Mol., Opt. Phys.*, 1996, **54**, 2146–2153.
80 T. D. Märk, *J. Chem. Phys.*, 1975, **63**, 3731–3736.
81 H. C. Straub, P. Renault, B. G. Lindsay, K. A. Smith and R. F. Stebbings, *Phys. Rev. A: At., Mol., Opt. Phys.*, 1995, **52**, 1115–1124.
82 S. J. King and S. D. Price, *Int. J. Mass Spectrom.*, 2008, **272**, 154–164.
83 C. Tian and C. R. Vidal, *Phys. Rev. A: At., Mol., Opt. Phys.*, 1998, **58**, 3783–3795.
84 T. Shirai, T. Tabata and H. Tawara, *At. Data Nucl. Data Tables*, 2001, **79**, 143–184.
85 W. E. Moddeman, T. A. Carlson, M. O. Krause, B. P. Pullen, W. E. Bull and G. K. Schweitzer, *J. Chem. Phys.*, 1971, **55**, 2317–2336.
86 D. A. Verner and D. G. Yakovlev, *Astron. Astrophys., Suppl. Ser.*, 1995, **109**, 125–133.
87 R. Spohr, T. Bergmark, N. Magnusson, L. O. Werme, C. Nordling and K. Siegbahn, *Phys. Scr.*, 1970, **2**, 31–37.
88 V. Feyer, P. Bolognesi, M. Coreno, K. C. Prince, L. Avaldi, L. Storchi and F. Tarantelli, *J. Chem. Phys.*, 2005, **123**, 224306–224308.
89 S. Svensson, A. N. Debrito, M. P. Keane, N. Correia, L. Karlsson, C. M. Liegener and H. Agren, *J. Phys. B: At., Mol. Opt. Phys.*, 1992, **25**, 135–144.
90 I. H. Suzuki and N. Saito, *Laser Chem.*, 1995, **16**, 5–18.
91 S. Svensson and L. Karlsson, *Phys. Scr.*, 1992, **41**, 132–142.
92 V. Ulrich, S. Barth, T. Lischke, S. Joshi, T. Arion, M. Mucke, M. Förstel, A. M. Bradshaw and U. Hergenhahn, *J. Electron Spectrosc. Relat. Phenom.*, 2011, **183**, 70–79.
93 Z. Bao, R. F. Fink, O. Travnikova, D. Céolin, S. Svensson and M. Novella Piancastelli, *J. Phys. B: At. Mol. Phys.*, 2008, **41**, 5101.
94 M. Larsson, P. Baltzer, S. Svensson, B. Wannberg and N. Martensson, *J. Phys. B: At., Mol. Opt. Phys.*, 1990, **23**, 1175–1195.
95 R. Püttner, V. Sekushin, G. Kaindl, X. J. Liu, H. Fukuzawa, K. Ueda, T. Tanaka, M. Hoshino and H. Tanaka, *J. Phys. B: At. Mol. Phys.*, 2008, **41**, 5103.
96 H. Kjeldsen, J. E. Hansen, F. Folkmann, H. Knudsen, J. B. West and T. Andersen, *Astrophys. J. Suppl.*, 2001, **135**, 285–295.
97 S. N. Nahar and A. K. Pradhan, *Astrophys. J. Suppl.*, 1997, **111**, 339.
98 H. Kjeldsen, B. Kristensen, R. L. Brooks, F. Folkmann, H. Knudsen and T. Andersen, *Astrophys. J. Suppl.*, 2002, **138**, 219–227.
99 A. Aguilar, A. M. Covington, G. Hinojosa, R. A. Phaneuf, I. Alvarez, C. Cisneros, J. D. Bozek, I. Dominguez, M. M. Sant'Anna, A. S. Schlachter, S. N. Nahar and B. M. McLaughlin, *Astrophys. J. Suppl.*, 2003, **146**, 467–477.
100 T. Andersen, H. Kjeldsen, H. Knudsen and F. Folkmann, *J. Phys. B: At., Mol. Opt. Phys.*, 2001, **34**, L327–L332.
101 L. Veseth, *J. Phys. B: At., Mol. Opt. Phys.*, 2001, **34**, L773–L777.
102 J. M. Bizau, personal communication.
103 D. A. Verner, D. G. Yakovlev, I. M. Band and M. B. Trzhaskovskaya, *At. Data Nucl. Data Tables*, 1993, **55**, 233–280.

View Article Online

Published on 19 September 2011. Downloaded by BELGIAN INSTITUTE FOR SPACE AERONOMY on 11/02/2016 11:00:19.

104 H. Tawara and M. Kato, *Electron Impact Ionization Data for Atoms and Ions—up-dated in 1998*, National Institute for Fusion Science, Nagoya, 1999.
105 I. Yamada, A. Danjo, T. Hirayama, A. Matsumoto, S. Ohtani, H. Suzuki, H. Tawara, T. Takayanagi, K. Wakiya and M. Yoshino, *J. Phys. Soc. Jpn.*, 1988, **57**, 2699.
106 D. S. Belic, D. J. Yu, A. Siari and P. Defrance, *J. Phys. B: At., Mol. Opt. Phys.*, 1997, **30**, 5535–5544.
107 H. Deutsch, K. Becker, P. Defrance, U. Onthong, M. Probst, S. Matt, P. Scheier and T. D. Mark, *Int. J. Mass Spectrom.*, 2003, **223**, 639–646.
108 H. Cherkani-Hassani, D. S. Belic, J. J. Jureta and P. Defrance, *J. Phys. B: At., Mol. Opt. Phys.*, 2006, **39**, 5105–5117.
109 I. Yamada, A. Danjo, T. Hirayama, A. Matsumoto, S. Ohtani, H. Suzuki, T. Takayanagi, H. Tawara, K. Wakiya and M. Yoshino, *J. Phys. Soc. Jpn.*, 1989, **58**, 3151.
110 E. M. Bahati, J. J. Jureta, D. S. Belic, S. Rachafi and P. Defrance, *J. Phys. B: At., Mol. Opt. Phys.*, 2001, **34**, 1757–1767.
111 E. Wells, V. Krishnamurthi, K. D. Carnes, N. G. Johnson, H. D. Baxter, D. Moore, K. M. Bloom, B. M. Barnes, H. Tawara and I. Ben-Itzhak, *Phys. Rev. A: At., Mol., Opt. Phys.*, 2005, **72**, 22726.
112 P. Bhatt, R. Singh, N. Yadav and R. Shanker, *Phys. Rev. A: At., Mol., Opt. Phys.*, 2010, **82**, 44702.
113 LPGP, GAPHYOR, http://gaphyor.lpgp.u-psud.fr/gaphyor/gaphyor.html.
114 R. A. Phaneuf, *Nucl. Fusion Spec. Suppl.*, 1992, **2**, 75.
115 Z. Fang and V. H. S. Kwong, *Astrophys. J.*, 1997, **474**, 529.
116 Z. Fang and V. H. S. Kwong, *Phys. Rev. A: At., Mol., Opt. Phys.*, 1997, **55**, 440–443.
117 P. Honvault, M. Gargaud, M. C. Bacchus-Montabonel and R. McCarroll, *Astron. Astrophys.*, 1995, **302**, 931.
118 Z. Fang and V. H. S. Kwong, *Phys. Rev. A: At., Mol., Opt. Phys.*, 1995, **51**, 1321–1326.
119 M. Kimura, J. P. Gu, G. Hirsch and R. J. Buenker, *Phys. Rev. A: At., Mol., Opt. Phys.*, 1996, **53**, 4164–4168.
120 R. Johnsen and M. A. Biondi, *Geophys. Res. Lett.*, 1978, **5**, 847–848.
121 M. S. Huq, R. L. Champion and L. D. Doverspike, *Phys. Rev. A: At., Mol., Opt. Phys.*, 1988, **37**, 2349–2353.
122 S. A. Rogers, S. D. Price and S. R. Leone, *J. Chem. Phys.*, 1993, **98**, 280–289.
123 A. Ehbrecht, N. Mustafa, C. Ottinger and Z. Herman, *J. Chem. Phys.*, 1996, **105**, 9833–9846.
124 W. Lu, P. Tosi and D. Bassi, *J. Chem. Phys.*, 2000, **112**, 4648–4651.
125 D. Mathur and F. A. Rajgara, *Phys. Rev. A: At., Mol., Opt. Phys.*, 1990, **41**, 4824.
126 B. K. Chatterjee and R. Johnsen, *J. Chem. Phys.*, 1989, **91**, 1378–1379.
127 M. A. Parkes, J. F. Lockyear, S. D. Price, D. Schröder, J. Roithova and Z. Herman, *Phys. Chem. Chem. Phys.*, 2010, **12**, 6233.
128 S. D. Price, S. A. Rogers and S. R. Leone, *J. Chem. Phys.*, 1993, **98**, 9455–9465.
129 M. P. Nakada and S. F. Singer, *Geophys. J. R. Astron. Soc.*, 1968, **15**, 163–181.
130 K. Seiersen, O. Heber, M. J. Jensen, C. P. Safvan and L. H. Andersen, *J. Chem. Phys.*, 2003, **119**, 839–843.
131 T. Kato and E. Asano, *Comparison of recombination rate coefficients given by empirical formulas for ions from Hydrogen through Nickel*, National Institute for Fusion Science, Nagoya, 1999.
132 K. Seiersen, A. Al-Khalili, O. Heber, M. J. Jensen, I. B. Nielsen, H. B. Pedersen, C. P. Safvan and L. H. Andersen, *Phys. Rev. A: At., Mol., Opt. Phys.*, 2003, **68**, 22708.
133 S. D. Price, personal communication.
134 D. Mathur, L. H. Andersen, P. Hvelplund, D. Kella and C. P. Safvan, *J. Phys. B: At., Mol. Opt. Phys.*, 1995, **28**, 3415–3426.
135 F. Mrugala, *J. Chem. Phys.*, 2008, **129**, 4314.
136 R. Bakova, J. Fiser, T. Sedivcova-Uhlikova and V. Spirko, *J. Chem. Phys.*, 2008, **128**, 4301.
137 D. Edvardsson, *Chem. Phys.*, 1998, **229**, 203–216.
138 H. D. Hagstrum and J. T. Tate, *Phys. Rev.*, 1941, **59**, 354–370.
139 H. Kjeldsen, *J. Phys. B: At., Mol. Opt. Phys.*, 2006, **39**, 325.
140 J. H. D. Eland, *Chem. Phys.*, 2006, **323**, 391–396.
141 M. W. Wong and L. Radom, *J. Am. Chem. Soc.*, 1989, **111**, 1155–1156.
142 R. Conrad, *Phys. Z.*, 1930, **31**, 888.
143 A. L. Vaughan, *Phys. Rev.*, 1931, **38**, 1687–1695.
144 D. Cossart and J. M. Robbe, *Chem. Phys. Lett.*, 1999, **311**, 248–254.
145 B. Mondal, N. C. Bera and A. K. Das, *Int. J. Quantum Chem.*, 2009, **109**, 469–476.
146 S. Hsieh and J. H. D. Eland, *J. Phys. B: At., Mol. Opt. Phys.*, 1996, **29**, 5795–5809.
147 M. Lundqvist, P. Baltzer, D. Edvardsson, L. Karlsson and B. Wannberg, *Phys. Rev. Lett.*, 1995, **75**, 1058–1061.
148 J. P. Bouhnik, I. Gertner, B. Rosner, Z. Amitay, O. Heber, D. Zajfman, E. Y. Sidky and I. Ben-Itzhak, *Phys. Rev. A: At., Mol., Opt. Phys.*, 2001, **63**, 32509.
149 T. Sedivcova, P. R. Zdanska, V. Spirko and J. Fiser, *J. Chem. Phys.*, 2006, **124**, 4303.
150 C. E. Melton and G. F. Wells, *J. Chem. Phys.*, 1957, **27**, 1132–1141.
151 J. J. Thomson, *Rays of Positive Electricity and their Application to Chemical Analysis*, Longmans Green and Co Ltd., London, 2nd edn, 1921.
152 G. Dawber, A. G. McConkey, L. Avaldi, M. A. MacDonald, G. C. King and R. I. Hall, *J. Phys. B: At., Mol. Opt. Phys.*, 1994, **27**, 2191–2209.
153 M. Hochlaf, R. I. Hall, F. Penent, H. Kjeldsen, P. Lablanquie, M. Lavollée and J. H. D. Eland, *Chem. Phys.*, 1996, **207**, 159–165.
154 J. Senekowitsch, S. Oneil, P. Knowles and H. J. Werner, *J. Phys. Chem.*, 1991, **95**, 2125–2127.
155 B. Brehm and G. Defrenes, *Int. J. Mass Spectrom. Ion Phys.*, 1978, **26**, 251–266.
156 E. Krishnakumar and S. K. Srivastava, *J. Phys. B: At., Mol. Opt. Phys.*, 1990, **23**, 1893–1903.
157 S. Halas and B. Adamczyk, *Int. J. Mass Spectrom. Ion Phys.*, 1972, **10**, 157–160.
158 M. Lundqvist, D. Edvardsson, P. Baltzer and B. Wannberg, *J. Phys. B: At., Mol. Opt. Phys.*, 1996, **29**, 1489–1499.
159 M. J. Besnard, L. Hellner and G. Dujardin, *J. Chem. Phys.*, 1988, **89**, 6554–6555.
160 A. Crowe and J. W. McConkey, *J. Phys. B: At. Mol. Phys.*, 1973, **6**, 2108–2117.
161 D. Cossart, F. Launay, J. M. Robbe and G. Gandara, *J. Mol. Spectrosc.*, 1985, **113**, 142–158.
162 D. Cossart and F. Launay, *J. Mol. Spectrosc.*, 1985, **113**, 159–166.
163 A. Ehresmann, H. Liebel, H. Schmoranzer, B. Zimmermann, S. Kammer, K. H. Schartner, P. V. Demekhin and V. L. Sukhorukov, *J. Phys. B: At., Mol. Opt. Phys.*, 2003, **36**, 3669–3681.
164 C. L. Ricketts, S. M. Harper, S. W. P. Hu and S. D. Price, *J. Chem. Phys.*, 2005, **123**, 4322.
165 J. T. Tate, P. T. Smith and A. L. Vaughan, *Phys. Rev.*, 1935, **48**, 525–531.
166 S. G. Cox, A. D. J. Critchley, P. S. Kreynin, I. R. McNab, R. C. Shiell and F. E. Smith, *Phys. Chem. Chem. Phys.*, 2003, **5**, 663–676.
167 M. J. Besnard, L. Hellner, Y. Malinovich and G. Dujardin, *J. Chem. Phys.*, 1986, **85**, 1316–1321.
168 D. Cossart, M. Bonneau and J. M. Robbe, *J. Mol. Spectrosc.*, 1987, **125**, 413–427.
169 D. Cossart and C. Cossart-Magos, *J. Mol. Spectrosc.*, 1991, **147**, 471–477.
170 F. Bennett, *Chem. Phys. Lett.*, 2003, **372**, 557–562.
171 T. Masuoka, *J. Chem. Phys.*, 1994, **100**, 6422–6428.
172 Z. Herman, *Chem. Phys.*, 1988, **126**, 377–384.
173 D. S. Waddell and R. K. Boyd, *Int. J. Mass Spectrom. Ion Processes*, 1989, **93**, 337–358.
174 M. W. Wong, R. H. Nobes, W. J. Bouma and L. Radom, *J. Chem. Phys.*, 1989, **91**, 2971–2979.
175 M. Lundqvist, D. Edvardsson, P. Baltzer, M. Larsson and B. Wannberg, *J. Phys. B: At., Mol. Opt. Phys.*, 1996, **29**, 499–514.
176 A. C. Hurley, *J. Mol. Spectrosc.*, 1962, **9**, 18–29.
177 N. H. F. Beebe, E. W. Thulstrup and A. Andersen, *J. Chem. Phys.*, 1976, **64**, 2080–2093.
178 M. Mahalingam and D. M. Hanson, *J. Chem. Phys.*, 1992, **97**, 2183–2188.

 This journal is © the Owner Societies 2011

View Article Online

Published on 19 September 2011. Downloaded by BELGIAN INSTITUTE FOR SPACE AERONOMY on 11/02/2016 11:00:19.

179 J. A. Samson and G. N. Haddad, *Phys. Rev. Lett.*, 1974, **33**, 875–878.
180 F. H. Dorman and J. D. Morrison, *J. Chem. Phys.*, 1961, **35**, 575–581.
181 V. Sharma, B. Bapat, J. Mondal, M. Hochlaf, K. Giri and N. Sathyamurthy, *J. Phys. Chem. A*, 2007, **111**, 10205–10211.
182 M. Hochlaf, F. R. Bennett, G. Chambaud and P. Rosmus, *J. Phys. B: At., Mol. Opt. Phys.*, 1998, **31**, 2163–2175.
183 M. Alagia, P. Candori, S. Falcinelli, M. Lavollée, F. Pirani, R. Richter, S. Stranges and F. Vecchiocattivi, *Phys. Chem. Chem. Phys.*, 2010, **12**, 5389.
184 P. Franceschi, R. Thissen, J. Zabka, J. Roithova, Z. Herman and O. Dutuit, *Int.J. Mass Spectrom.*, 2003, **228**, 507–516.
185 J. Zabka, C. L. Ricketts, D. Schroder, J. Roithova, H. Schwarz, R. Thissen, O. Dutuit, S. D. Price and Z. Herman, *J. Phys. Chem. A*, 2010, **114**, 6463–6471.
186 J. Roithova and D. Schröder, *Phys. Chem. Chem. Phys.*, 2007, **9**, 2341–2349.
187 H. Balsiger, K. Altwegg, P. Bochsler, P. Eberhardt, J. Fischer, S. Graf, A. Jäckel, E. Kopp, U. Langer, M. Mildner, J. Müller, T. Riesen, M. Rubin, S. Scherer, P. Wurz, S. Wüthrich, E. Arijs, S. Delanoye, J. de Keyser, E. Neefs, D. Nevejans, H. Rème, C. Aoustin, C. Mazelle, J. L. Médale, J. A. Sauvaud, J. J. Berthelier, J. L. Bertaux, L. Duvet, J. M. Illiano, S. A. Fuselier, A. G. Ghielmetti, T. Magoncelli, E. G. Shelley, A. Korth, K. Heerlein, H. Lauche, S. Livi, A. Loose, U. Mall, B. Wilken, F. Gliem, B. Fiethe, T. I. Gombosi, B. Block, G. R. Carignan, L. A. Fisk, J. H. Waite, D. T. Young and H. Wollnik, *Space Sci. Rev.*, 2007, **128**, 745–801.
188 S. Shiki, M. Ukibe, Y. Sato, S. Tomita, S. Hayakawa and M. Ohkubo, *J. Mass Spectrom.*, 2008, **43**, 1686–1691.
189 F. P. Keenan, *Space Sci. Rev.*, 1996, **75**, 537–550.
190 P. K. Carroll, *Can. J. Phys.*, 1958, **36**, 1585.
191 D. Cossart, C. Cossartmagos and F. Launay, *J. Chem. Soc., Faraday Trans.*, 1991, **87**, 2525–2528.
192 J. Bishop and P. D. Feldman, *J. Geophys. Res.*, 2003, **108**, 1243.
193 J. M. Ajello, M. H. Stevens, I. Stewart, K. Larsen, L. Esposito, J. Colwell, W. McClintock, G. Holsclaw, J. Gustin and W. Pryor, *Geophys. Res. Lett.*, 2007, **34**, L24204–L24208.
194 M. H. Stevens, J. Gustin, J. M. Ajello, J. S. Evans, R. R. Meier, A. J. Kochenash, A. W. Stephan, A. I. F. Stewart, L. W. Esposito, W. E. McClintock, G. Holsclaw, E. T. Bradley, B. R. Lewis and A. N. Heays, *J. Geophys. Res.*, 2011, **116**, 05304.
195 C. A. Nicolaides, *Chem. Phys. Lett.*, 1989, **161**, 547–553.
196 V. G. Nenajdenko, N. E. Shevchenko, E. S. Balenkova and I. V. Alabugin, *Chem. Rev.*, 2003, **103**, 229–282.
197 D. Mathur, *Phys. Rep.*, 2004, **391**, 1–118.
198 S. D. Price, *Phys. Chem. Chem. Phys.*, 2003, **5**, 1717–1729.
199 J. Roithova and D. Schröder, *Phys. Chem. Chem. Phys.*, 2007, **9**, 731–738.
200 J. Roithova and D. Schröder, *Chem.–Eur. J.*, 2007, **13**, 2893–2902.
201 J. L. Fox and F. M. Bakalian, *J. Geophys. Res.*, 2001, **106**, 28785–28796.
202 J. L. Fox and A. B. Hac, *Icarus*, 2009, **204**, 527–544.
203 R. E. Johnson, M. R. Combi, J. L. Fox, W. H. Ip, F. Leblanc, M. A. McGrath, V. I. Shematovich, D. F. Strobel and J. H. Waite, *Space Sci. Rev.*, 2008, **139**, 355–397.
204 J. H. Waite, S. Lewis, W. T. Kasprzak, V. G. Anicich, B. P. Block, T. E. Cravens, G. G. Fletcher, W. H. Ip, J. G. Luhmann, R. L. McNutt, H. B. Niemann, J. K. Parejko, J. E. Richards, R. L. Thorpe, E. M. Walter and R. V. Yelle, *Space Sci. Rev.*, 2004, **114**, 113–231.
205 J. Cui, R. V. Yelle, V. Vuitton, J. H. Waite, W. T. Kasprzak, D. A. Gell, H. B. Niemann, I. C. F. Müller-Wodarg, N. Borggren, G. G. Fletcher, E. L. Patrick, E. Raaen and B. A. Magee, *Icarus*, 2009, **200**, 581–615.
206 M. Hochlaf, A. Pilcher-Clayton and J. H. D. Eland, *Chem. Phys.*, 2005, **309**, 291–301.
207 S. Barabash, J. A. Sauvaud, H. Gunell, H. Andersson, A. Grigoriev, K. Brinkfeldt, M. Holmström, R. Lundin, M. Yamauchi, K. Asamura, W. Baumjohann, T. L. Zhang, A. J. Coates, D. R. Linder, D. O. Kataria, C. C. Curtis, K. C. Hsieh, B. R. Sandel, A. Fedorov, C. Mazelle, J. J. Thocaven, M. Grande, H. E. J. Koskinen, E. Kallio, T. Säles, P. Riihela, J. Kozyra, N. Krupp, J. Woch, J. Luhmann, S. McKenna-Lawlor, S. Orsini, R. Cerulli-Irelli, M. Mura, M. Milillo, M. Maggi, E. Roelof, P. Brandt, C. T. Russell, K. Szego, J. D. Winningham, R. A. Frahm, J. Scherrer, J. R. Sharber, P. Wurz and P. Bochsler, *Planet. Space Sci.*, 2007, **55**, 1772–1792.
208 L. W. Esposito, C. A. Barth, J. E. Colwell, G. M. Lawrence, W. E. McClintock, A. I. F. Stewart, H. U. Keller, A. Korth, H. Lauche, M. C. Festou, A. L. Lane, C. J. Hansen, J. N. Maki, R. A. West, H. Jahn, R. Reulke, K. Warlich, D. E. Shemansky and Y. L. Yung, *Space Sci. Rev.*, 2004, **115**, 299–361.